



This discussion paper is/has been under review for the journal Atmospheric Chemistry and Physics (ACP). Please refer to the corresponding final paper in ACP if available.

A multi-year study of lower tropospheric aerosol variability and systematic relationships from four North American regions

J. P. Sherman¹, P. J. Sheridan², J. A. Ogren², E. A. Andrews², L. Schmeisser²,
A. Jefferson², and S. Sharma³

¹Dept. Physics and Astronomy, Appalachian State University, 525 Rivers St, CAP Building Room 231, Boone, NC, 28608, USA

²NOAA, Earth Systems Research Laboratory, Global Monitoring Division/GMD-1, 325 Broadway, Boulder, CO, 80305, USA

³Environment Canada, 4905 Dufferin St, Toronto, ON, M3H 5T4, Canada

Received: 28 September 2014 – Accepted: 10 October 2014 – Published: 28 October 2014

Correspondence to: J. P. Sherman (shermanjp@appstate.edu)

Published by Copernicus Publications on behalf of the European Geosciences Union.

A multi-year study of lower tropospheric aerosol variability and systematic relationships

J. P. Sherman et al.

Title Page

Abstract

Introduction

Conclusions

References

Tables

Figures



Back

Close

Full Screen / Esc

Printer-friendly Version

Interactive Discussion



Abstract

Hourly-averaged aerosol radiative properties measured over the years 2010–2013 at four continental North American NOAA/ES&F Federated Aerosol Network sites – Southern Great Plains in Lamont, OK (SGP), Bondville, IL (BND), Appalachian State University in Boone, NC (APP), and Egbert, Ontario, Canada (EGB) were analyzed to determine regional variability and temporal variability on several timescales, how this variability has changed over time at the long-term sites (SGP and BND), and whether systematic relationships exist for key aerosol properties relevant to radiative forcing calculations. The aerosol source types influencing the four sites differ enough so as to collectively represent rural, anthropogenically-perturbed air conditions over much of continental North America.

Seasonal variability in scattering and absorption coefficients at 550 nm (σ_{sp} and σ_{ap} , respectively) and most aerosol intensive properties was much larger than day of week and diurnal variability at all sites for both the sub-10 μm and sub-1 μm aerosols. Pronounced summer peaks in scattering were observed at all sites, accompanied by broader peaks in absorption, higher single-scattering albedo (ω_0), and lower hemispheric backscatter fraction (b). Amplitudes of diurnal and weekly cycles in absorption at the sites were larger for all seasons than those of scattering. The cycle amplitudes of intensive optical properties on these shorter timescales were minimal in most cases. In spite of the high seasonality in ω_0 and b , the co-variation of these two intensive properties cause the corresponding seasonal cycle in monthly median direct radiative forcing efficiency to be small, with changes of only a few percent at all sites.

Median sub-10 μm aerosol σ_{sp} values for SGP and BND for the 2010–2013 time period were $\sim 25\%$ lower for all months than during the late 1990s period studied by Delene and Ogren (2002), consistent with the trends reported in other North American studies. There were even larger reductions in sub-1 μm aerosol σ_{sp} , leading to a larger coarse-mode influence at both sites. Similar reductions in median σ_{ap} were observed at BND but median σ_{ap} changed little at SGP relative to the earlier observations of

A multi-year study of lower tropospheric aerosol variability and systematic relationships

J. P. Sherman et al.

Title Page

Abstract

Introduction

Conclusions

References

Tables

Figures

◀

▶

◀

▶

Back

Close

Full Screen / Esc

Printer-friendly Version

Interactive Discussion

D&O2002, leading to lower ω_0 at SGP. Most intensive properties and their variability were similar for both periods but median b was larger for all months of the 2010–2013 period at BND and nearly all months at SGP, indicating a shift toward smaller accumulation-mode particles.

Systematic relationships between aerosol radiative properties were developed and applied to provide information on aerosol source types and processes at the four sites but some key relationships varied noticeably with season, indicating that the use of such relationships for model evaluation and inversion of remote sensing data must consider their seasonality.

1 Introduction

Predictions of future climate change resulting from projected increases in carbon dioxide are limited primarily by large uncertainties in the direct and indirect radiative forcing due to aerosols (Andreae et al., 2005). On a global average, the measurement-based estimates of aerosol direct radiative forcing (DRF) are 55–80 % greater than the model-based estimates (Yu et al., 2009). The differences are even larger on regional scales and for the anthropogenic component (Yu et al., 2009). Such measurement-model discrepancies are the result of a combination of differences in aerosol amount, single-scattering albedo, surface albedo, and radiative transfer schemes (Yu et al., 2006). One of the high-priority tasks recommended to reduce the uncertainty in aerosol radiative effects is to “Maintain, enhance, and expand the surface observation networks measuring aerosol optical properties for satellite retrieval validation, model evaluation, and climate change assessments” (Kahn et al., 2009).

Studies based on continuous measurements made by global surface-based aerosol monitoring networks such as NASA’s Aerosol Robotic Network (AERONET, Holben et al., 1998) and NOAA’s Earth System Research Laboratory (NOAA/ESRL, Delene and Ogren, 2002) have contributed to improved understanding of mean values, spatial and temporal variability, and trends of aerosol loading and optical properties, in

A multi-year study of lower tropospheric aerosol variability and systematic relationships

J. P. Sherman et al.

Title Page

Abstract

Introduction

Conclusions

References

Tables

Figures



Back

Close

Full Screen / Esc

Printer-friendly Version

Interactive Discussion



A multi-year study of lower tropospheric aerosol variability and systematic relationships

J. P. Sherman et al.

Title Page

Abstract

Introduction

Conclusions

References

Tables

Figures

◀

▶

◀

▶

Back

Close

Full Screen / Esc

Printer-friendly Version

Interactive Discussion

5 addition to relationships among some of these properties, the US-based Interagency Monitoring of Protected Visual Environments network (IMPROVE, Malm et al., 2004) has conducted similar studies using speciated aerosol mass concentrations, light scattering (at some sites), and reconstructed light extinction measurements in remote areas
 10 of the US. Recent long-term trend studies based on data from surface networks indicate that aerosol optical depth (Li et al., 2014; Yoon, 2012) and lower tropospheric light scattering (Collaud-Coen et al., 2013) have decreased at a majority of North American aerosol monitoring sites. Hand et al. (2014) reported large reductions of up to 50 % in reconstructed aerosol visible light extinction for the 20 % haziest days annually at IMPROVE sites in the US from 2002–2011, with the largest decreases in the eastern US. Through trend analysis of speciated aerosol mass concentrations and emissions inventories, they showed that reductions in SO₂ emissions (produced largely by coal-burning power plants) have likely played a major role in the reduced aerosol light extinction, particularly in the eastern US. Murphy et al. (2011) applied trend analysis using IMPROVE sites across the US to show that elemental carbon aerosol mass concentrations decreased by over 25 % between 1990–2004, with reductions during winter months close to 50%. Region and season-dependent changes in emissions of aerosols and precursor gases may result in changes in mean values and variability of aerosol optical and micro-physical properties, but few long-term studies of aerosol intensive properties (i.e., properties that are independent of aerosol loading, such as single scattering albedo, asymmetry parameter, and direct radiative forcing efficiency) conducted over multiple regions have ever been performed in North America.

25 Surface-based networks employing in situ methods, such as the NOAA/ESRL Federated Aerosol Network, are particularly well-suited for studies of aerosol variability on a variety of temporal scales under both clear and cloudy conditions. An additional advantage is the ability to derive single-scattering albedo (ω_0) under low aerosol loading conditions. Single-scattering albedo derived from sky radiance measurements made by Cimel sun/sky radiometers as part of AERONET possess high uncertainties for lower aerosol optical depths typical of most rural North American sites (Dubovik et al., 2000).

A multi-year study of lower tropospheric aerosol variability and systematic relationships

J. P. Sherman et al.

Title Page

Abstract

Introduction

Conclusions

References

Tables

Figures

◀

▶

◀

▶

Back

Close

Full Screen / Esc

Printer-friendly Version

Interactive Discussion

A weakness of many in situ surface aerosol measurement systems is the inability to determine the hygroscopic dependence of aerosol light scattering. Many aerosol monitoring stations in the NOAA/ESRL and Global Atmosphere Watch (GAW) networks follow similar sampling protocols where the aerosols are dried to decouple the aerosol properties from their dependence on relative humidity (RH). Another concern is the uncertainty as to when and under what conditions the near-surface measurements are representative of the atmospheric column at each site. The first problem can be addressed through the use of humidified light scattering measurements (e.g., Sheridan et al., 2001), which are or have been made at a few ESRL network sites, including three of the four sites reported in this paper. The second issue has been investigated through multi-year aircraft measurement programs over instrumented surface sites. At the Southern Great Plains (SGP, near Lamont, OK) and Bondville (BND), IL sites respectively, Andrews et al. (2004) and Sheridan et al. (2012) have reported that median values of key dried aerosol intensive optical properties such as ω_0 and scattering Ångström exponent (α_{sp}) show little statistical variability up to ~ 2 km altitude and that long-term median values can be well-approximated by the near-surface values, even though instantaneous measurements of the near-surface properties are often poorly correlated with those of the column.

Delene and Ogren (2002) (hereafter referred to as D&O2002) reported multi-year measurements of aerosol optical properties at four North American sites that were used to (1) highlight the need to quantify both aerosol extensive properties (i.e., properties that depend on aerosol amount) and intensive properties on regional scales over at least a 1 year period; and (2) conclude that global measurements of aerosol optical depth (denoted by AOD or τ) made daily by satellites, combined with in situ measurements of regionally-representative aerosol intensive properties, are likely sufficient to determine aerosol direct radiative forcing with a relatively small amount of uncertainty. One drawback of their study was the then lack of NOAA/ESRL Federated Network sites in the eastern portion of North America, where population and aerosol loading is highest. D&O2002 also studied systematic relationships between aerosol

loading (using scattering coefficient as a proxy) and other optical properties. These relationships are particularly useful when only a subset of aerosol measurements are available. D&O2002 argued the importance of such relationships for the inversion of remote sensing data, whereby a dynamic model (applied by Remer and Kaufman, 1998) could be used to specify the constraining aerosol properties as a function of aerosol loading.

The study described here utilized four years (2010–2013) of continuous measurements of hourly-averaged aerosol light scattering, hemispheric backscattering, and light absorption made at four continental North American sites in the NOAA/ESRL Federated Aerosol Network: (i) SGP – located in the southern plains of the US, (ii) BND – located in the agricultural midwestern US, (iii) the Appalachian Atmospheric Interdisciplinary Research facility at Appalachian State University (APP) in Boone, NC – located in the southern Appalachian mountain region of the southeastern US, and (iv) the Environment Canada monitoring station at Egbert, Ontario (EGB) – located in the Canadian farmlands north/northwest of Toronto. These measurements were used to derive several key aerosol properties (Table 1) relevant to aerosol radiative forcing. Measurements from SGP and BND over 1997–2009 and 1996–2009, respectively, were also used to provide long-term context to the most recent four-year period and for comparison with results presented in D&O2002. Measured and derived aerosol properties were used to answer the following research questions:

1. How do key lower tropospheric aerosol optical properties differ among the four North American continental regions and how do they vary on different timescales (seasonal, weekly, diurnal) for each region? What do the observed spatial and temporal differences imply in terms of dominant sources and processes?
2. How have the magnitude and variability of aerosol optical properties changed at the long-term sites (SGP and BND) since D&O2002? What does this imply in terms of possible changes in sources and processes in these regions?

A multi-year study of lower tropospheric aerosol variability and systematic relationships

J. P. Sherman et al.

Title Page

Abstract

Introduction

Conclusions

References

Tables

Figures

◀

▶

◀

▶

Back

Close

Full Screen / Esc

Printer-friendly Version

Interactive Discussion



3. Are there systematic relationships between these optical properties? How do these relationships vary with region and with season?

This study differs from the D&O2002 paper in three respects:

1. The time period of the study is different, which allows for us to compare (at least for BND and SGP) how the optical properties have changed.
2. This paper has a focus on continental sites, whereas D&O2002's four sites included an Arctic site and a marine site.
3. Aerosol temporal variability and systematic relationships between aerosol optical properties are investigated as a function of season. D&O2002 only looked at annual systematic variability.

2 Methodology

2.1 Site descriptions

All four sites in this study are mid-latitude (35–45° N) locations in North America with elevations ranging from 230 to 1080 m a.s.l., placing them firmly in the boundary layer. These sites can be categorized as anthropogenically-perturbed, rural continental locations, distant from both large population centers and significant emissions sources and thus representative of regional atmospheric conditions. BND is located near a regional population center (Sect. 2.1.3) that lies predominately downwind of the site, justifying the same categorization as the other sites. Table 2 and the sections below provide additional details about each location.

2.1.1 Lamont, Oklahoma, USA (SGP)

SGP is the Department of Energy's Cloud, Aerosol and Radiation Testbed (CART) site and is located in north central Oklahoma near the town of Lamont (pop. 417) in

26977

ACPD

14, 26971–27038, 2014

A multi-year study of lower tropospheric aerosol variability and systematic relationships

J. P. Sherman et al.

Title Page

Abstract

Introduction

Conclusions

References

Tables

Figures

◀

▶

◀

▶

Back

Close

Full Screen / Esc

Printer-friendly Version

Interactive Discussion



A multi-year study of lower tropospheric aerosol variability and systematic relationships

J. P. Sherman et al.

Title Page

Abstract

Introduction

Conclusions

References

Tables

Figures

◀

▶

◀

▶

Back

Close

Full Screen / Esc

Printer-friendly Version

Interactive Discussion

5 a rural, agricultural region surrounded mostly by wheat, corn and soybean fields. Measurements of in situ aerosol optical properties began in 1996. The sub-1 μm aerosol composition is mostly organic with varying amounts of sulfate and nitrates (Fast et al., 2014). The super-1 μm aerosol includes dust, particularly during dry seasons and high
10 wind episodes. Biomass burning aerosol from crop and grass fires is present often in the late spring and fall (Kohler et al., 2011). Emissions from a local oil refinery and power plant occasionally impact the site (Sheridan et al., 2001). More recently gas and oil drilling activity has increased in the region with several “fracking” sites close to the facility. The site is also equipped with a Cimel sunphotometer as part of AERONET,
15 cloud radars, lidars, meteorological instruments and many remote-sensing radiometers, making it the largest climate research facility in the world. Climatologies of surface and aerosol optical properties observed at SGP have been reported by Sheridan et al. (2001) and D&O2002.

2.1.2 Bondville, Illinois, USA (BND)

15 The BND aerosol monitoring system is located on farmland at the Bondville Environmental and Atmospheric Research Site (BEARS) in central Illinois. In situ aerosol measurements at BND began in 1994. The station is located approximately 6.5 km south of Bondville, IL (pop. 450), 16 km southwest of Champaign–Urbana (population ~ 230 000), and is surrounded by corn, soybean and hay fields. The prevailing wind
20 directions at the station cover a range from S to WNW (i.e., predominantly upwind of the nearby towns). Climatologies of surface aerosol optical properties observed at BND have been reported by Koloutsou-Vakakis et al. (2001) and D&O2002. Sheridan et al. (2012) reported BND surface aerosol properties for comparison with their airborne aerosol measurements. The sub-1 μm aerosol is comprised primarily of ammonium,
25 sulfate, organic and elemental carbon (Koloutsou-Vakakis et al., 2001). Additional measurements made at BND include a Cimel sunphotometer as part of AERONET, meteorological instruments, an IMPROVE aerosol chemistry system, and a full suite of solar radiation measurements made by the NOAA/ESRL Global Monitoring Division.

2.1.3 Egbert, Ontario, Canada (EGB)

The Center for Atmospheric Research Experiments (CARE) is situated on agricultural land near the hamlet of Egbert, approximately 75 km NNW of Toronto, Ontario, with both forests and farmland nearby. The population of Egbert and surrounding communities is approximately 20 000. Air arriving from the north is generally much cleaner than air from the south, which is influenced by the densely populated southern Ontario region and the northeastern US. Measurements of sub-1 μm aerosol chemistry have higher sulfate, black carbon, and organics in arriving from the south while cleaner north and westerly air masses are mostly dominated by organics of biogenic influence (Chan et al., 2010), especially during the late spring summer, and early fall. There are measurements of greenhouse gases such as CO_2 , CH_4 , and SF_6 at this location, in addition to aerosol chemistry and size distribution and various meteorological measurements.

2.1.4 Appalachian State University, Boone, North Carolina, USA (APP)

The APP site is situated at the highest point on the Appalachian State University campus, located in the Southern Appalachian mountain town of Boone, NC (pop. $\sim 20\,000$). The region surrounding Boone is heavily forested. In situ aerosol measurements were initiated in June 2009. APP is also home to a Cimel sunphotometer as part of AERONET, a micro-pulsed lidar, an aerosol mass spectrometer, a solar pyranometer as part of the NASA SolRad-Net, and a suite of meteorological and trace gas measurements. The lower tropospheric sub-1 μm aerosol mass measured at APP consists primarily of organics, with lower levels of sulfates (Fig. S1 of Supplement tied to this paper). Both warm-season and cold-season organic aerosol mass fractions consist largely of highly oxidized, “aged” aerosol (low-volatility, oxygenated OA; LV-OOA) indicative of regional background aerosol (Link et al., 2014). Summer aerosol optical depth in the warm, heavily-forested SE US is heavily influenced by isoprene-derived organic aerosol (Goldstein et al., 2009). A biomass-burning influence was also present in

A multi-year study of lower tropospheric aerosol variability and systematic relationships

J. P. Sherman et al.

Title Page

Abstract

Introduction

Conclusions

References

Tables

Figures

◀

▶

◀

▶

Back

Close

Full Screen / Esc

Printer-friendly Version

Interactive Discussion

winter aerosol mass concentrations measured at APP (Link et al., 2014). Wood-burning is a common heating fuel in the Southern Appalachians.



2.1.5 Air sampling infrastructure at the sites



All of the sites were designed with similar inlet systems following established NOAA/ESRL and GAW aerosol sampling protocols (Sheridan et al., 2001). To minimize contamination from local activities around the stations, ambient aerosols were sampled from the top of sampling stacks that were at least 10 m above the surrounding terrain. For BND, EGB, and SGP, this was 10 m above the ground since the immediate surrounding areas were not forested. For APP, the sampling inlet was at the top of a 34 m tall tower, which was necessary to sample at a level above the surrounding trees. To reduce the confounding effects of RH on the aerosol measurements, the sample air was gently heated at all sites except EGB to achieve sample line and instrument RH $\leq 40\%$ for a very large majority of hours at these sites. Elevated instrument temperatures (relative to ambient air) at EGB resulted in instrument RH that was typically well below ambient RH, although still above 40% for some hours. Based on our analysis outlined in Sect. 2.3, aerosol measurements at EGB are also believed to be representative of low-RH conditions.

All of the sites except EGB used a switched impactor system (e.g., Sheridan et al., 2001) to alternate between sub-10 μm ($D_p < 10 \mu\text{m}$) and sub-1 μm ($D_p < 1 \mu\text{m}$) aerodynamic diameter particle size ranges. In this paper, these size cut ranges will be referred to using the common convention PM_{10} and PM_1 , respectively, where PM is the acronym for *particulate matter*. APP and SGP size-cut switching occurs every 15 and 30 min, respectively, in order to facilitate ramping of the RH in the humidograph system used to measure the hygroscopic dependence of light scattering (humidograph data are not presented in this study). BND size-cut switching occurs every six minutes. In this study, hourly-averaged data are used. With the exception of short-lived plumes of local influence (which are removed by the site scientist as part of data quality assurance), aerosol concentrations and properties at the sites typically show little change on

A multi-year study of lower tropospheric aerosol variability and systematic relationships

J. P. Sherman et al.

Title Page

Abstract

Introduction

Conclusions

References

Tables

Figures



Back

Close

Full Screen / Esc

Printer-friendly Version

Interactive Discussion



timescales less than one hour so it is assumed that the same aerosols are sampled for both size cuts at these switching rates over a large majority of hours. The EGB system used a 1 μm URG cyclone to achieve a permanent $D_p < 1 \mu\text{m}$ particle size cut so PM_{10} aerosol properties are not available for EGB. Descriptions of the basic inlet design and sampling strategy, including flow rates, tubing sizes and estimated aerosol losses, have been provided elsewhere (Sheridan et al., 2001; D&O2002).

2.2 Measurements and instruments

This study used several primary aerosol measurements (Table 2), including aerosol light scattering (σ_{sp}), hemispheric backscattering (σ_{bsp}), and absorption (σ_{ap}) coefficients. All of these parameters were measured for both the PM_{10} and PM_1 size ranges (only PM_1 for EGB) so that the fractional radiative effects of sub-1 μm particles (PM_1) could be estimated.

A three-wavelength ($3\text{-}\lambda$) integrating nephelometer (Model 3563, TSI Inc., St. Paul, MN) was used at all sites for measurement of the total light scattering coefficients (angular range of 7–170°) and hemispheric backscattering coefficients (angular range of 90–170°). The operating wavelengths for the instruments used in this study are given in Table 2. Measurement details and uncertainties for the TSI nephelometer have been described elsewhere (e.g., Anderson et al., 1999; Sheridan et al., 2002). Aerosol properties at these locations (e.g., $\omega_0 > 0.7$ and minor coarse mode fractions, as discussed by Massoli et al., 2009) were such that the widely-used nephelometer correction (e.g., truncation) scheme of Anderson and Ogren (1998) was considered appropriate and applied in this study.

The aerosol light absorption coefficients were determined with filter-based instruments that make measurements at wavelengths close to those of the TSI nephelometer. The majority of these measurements were made with 3- λ Particle Soot Absorption Photometers (PSAP, Radiance Research, Seattle, WA). PSAP measurements were corrected for sample area, flow rate, and non-idealities in the manufacturer's calibration as described in Bond et al. (1999) and Ogren (2010). Measurement uncertainties for

A multi-year study of lower tropospheric aerosol variability and systematic relationships

J. P. Sherman et al.

Title Page

Abstract

Introduction

Conclusions

References

Tables

Figures

◀

▶

◀

▶

Back

Close

Full Screen / Esc

Printer-friendly Version

Interactive Discussion



A multi-year study of lower tropospheric aerosol variability and systematic relationships

J. P. Sherman et al.

[Title Page](#)[Abstract](#)[Introduction](#)[Conclusions](#)[References](#)[Tables](#)[Figures](#)[◀](#)[▶](#)[◀](#)[▶](#)[Back](#)[Close](#)[Full Screen / Esc](#)[Printer-friendly Version](#)[Interactive Discussion](#)

the PSAP have been described in detail elsewhere (Anderson et al., 1999; Bond et al., 1999; Sheridan et al., 2002). The EGB station was an exception in that it had a single wavelength (1- λ) PSAP instrument operating continuously over its entire data record. Absorption Ångström exponent values were used to adjust the PSAP light absorption measurements to the nephelometer wavelengths for calculating intensive aerosol properties (Table 1). The PSAPs were modified by placing a small (~ 5 W) heater on their internal inlet lines at the connection with the optical block. The heating was gentle, typically only a few degrees, but the temperature of the metal block was kept elevated above the incoming sample air temperature so the RH of the sample and reference filters stayed relatively low. The heater was not actively controlled to maintain a specific RH, but RH variability at low RH is not believed to influence the measurements as strongly as RH variability at high RH (Anderson et al., 2003). Tests suggest that the heater kept the RH at the filters below 40 % most of the time. An RH of 50 % at the filter would have been exceeded only during sampling of very humid air (Sheridan et al., 2012).

A new light absorption instrument (Continuous Light Absorption Photometer, CLAP) was recently developed by NOAA/ESRL to eventually replace the PSAP at all stations in the NOAA network (Ogren et al., 2013). The CLAP is similar to the PSAP in that particles are collected on a filter of the same material as used in the PSAP and light transmission through the filter is monitored continuously. The CLAP differs from the PSAP in that instead of a single sample spot, it has eight sample spots, which are selected by solenoids that switch to the next sample spot once the filter transmittance reaches a desired limit (typically 0.7). Thus, the CLAP can run eight times as long as the PSAP before requiring a filter change, ideal for remote sites which aren't visited daily or for highly polluted sites. The designed similarity with the PSAP means that the same corrections (Bond et al., 1999; Ogren, 2010) can be applied. After running for an extended overlap period with the CLAP at the BND station, the PSAP was removed in March 2012, so the final 21 months of light absorption measurements at BND were made with a CLAP. The PSAP/CLAP comparisons made during the overlap period at

A multi-year study of lower tropospheric aerosol variability and systematic relationships

J. P. Sherman et al.

Title Page

Abstract

Introduction

Conclusions

References

Tables

Figures

◀

▶

◀

▶

Back

Close

Full Screen / Esc

Printer-friendly Version

Interactive Discussion

BND indicate that the CLAP measures light absorption at all wavelengths about 5% lower on average than the PSAP. The CLAP comes with a small heater built in and is controlled to a set temperature, typically 39 °C to minimize RH effects during sampling.

The primary measurements (Table 2) such as σ_{sp} , σ_{bsp} , and σ_{ap} were used to derive several aerosol properties (Table 1) used in radiative transfer calculations (Haywood and Shine, 1995) and other aerosol studies. These properties have been described in many previous papers (e.g., Sheridan et al., 2001; D&O2002) so only a brief discussion follows. The light extinction coefficient (σ_{ep}) is the sum of the scattering and absorption coefficients. The primary measurements (plus σ_{ep}) are extensive parameters, as they depend on the amount of aerosol present. The single-scattering albedo (ω_0) is the fraction of extinction due to scattering, with lower values of ω_0 corresponding to more absorbing aerosols. The hemispheric backscatter coefficient (b) represents the fraction of light scattered into the backward hemisphere in the nephelometer and provides qualitative information on aerosol size, with larger values of b most often corresponding to smaller particles. The scattering and absorption Ångström exponents (α_{sp} and α_{ap}) describe the wavelength dependence of light scattering and absorption, respectively. The scattering Ångström exponent ($0 \leq \alpha_{sp} \leq 4$) provides semi-quantitative information regarding the aerosol size distribution, with larger values of α_{sp} corresponding to size distributions dominated by smaller particles (van de Hulst, 1957). The absorption Ångström exponent can provide information on aerosol type for certain aerosols (e.g., Costabile et al., 2013; Bergstrom et al., 2007). For example, dust and some organics absorb light strongly in the near-UV and blue-violet regions of the electromagnetic spectrum (the so-called “brown carbon”), corresponding to $\alpha_{ap} > 1$ (Costabile et al., 2013). Absorption by black carbon (BC) decreases as λ^{-1} in the near-UV through near-IR, corresponding to $\alpha_{ap} = 1$ (Bergstrom et al., 2007). The sub-1 μm scattering and absorption fractions R_{sp} and R_{ap} , respectively, indicate the fractions of PM₁₀ light scattering and absorption due to PM₁ particles and serve as a rough proxy for the “fine-mode” fraction of scattering and absorption. Haywood and Shine (1995) present simple equations for calculating top-of-atmosphere (TOA) aerosol direct radiative forc-

A multi-year study of lower tropospheric aerosol variability and systematic relationships

J. P. Sherman et al.

Title Page

Abstract

Introduction

Conclusions

References

Tables

Figures

◀

▶

◀

▶

Back

Close

Full Screen / Esc

Printer-friendly Version

Interactive Discussion



ing (DRF) and direct radiative forcing efficiency (DRFE, Table 1) for an optically-thin, partially-absorbing atmosphere. DRFE represents the DRF per unit aerosol optical depth (referenced in the literature as AOD or τ) and is to first-order independent of τ . If globally-averaged values for all non-aerosol parameters are used (Table 1), the simple equation for DRFE provides a means of comparing the intrinsic forcing efficiency of the aerosols measured at different sites and times, through its dependence on ω_0 and on up-scatter fraction β . The up-scatter fraction represents the fraction of incoming solar radiation that is scattered by atmospheric aerosols back to space, and has been related to the measured parameter b by the approximation of Wiscombe and Grams (1976). A second-order curve fit of the points in their Fig. 3 as reported in Sheridan and Ogren (1999) provides the parameterization shown in Table 1.

2.3 Data consistency



Quality assurance for each site was performed by the site scientist to invalidate measurements affected by instrumental or sampling problems and to eliminate data contaminated by local sources (e.g., short-lived plumes caused by local traffic sources, mowing operations, etc.). Data where the PSAP filter transmission was less than 50 % were also discarded because high filter loading greatly increases the measurement uncertainty (Bond et al., 1999). Details of the quality assurance methods are provided in D&O2002. In addition to being measured at low RH, the scattering and absorption measurements were adjusted to standard temperature and pressure ($T = 273.15$ K, $P = 101.35$ kPa) to facilitate comparisons among the sites. Only hours for which scattering at 550 nm was at least 1.0 M m^{-1} for the PM_{10} size cut were used to calculate the aerosol intensive property statistics, so as to reduce noise resulting from taking ratios of two small quantities (see Table 1). This filtering discarded 1 % or fewer of the hours at all sites except SGP, where 3.9 % of the hours were discarded. The lack of PM_{10} data from EGB precluded calculation of sub- $1 \mu\text{m}$ aerosol scattering and absorption fractions R_{sp} and R_{ap} and the use of a single-wavelength PSAP at EGB precluded calculation of absorption Ångström exponent (α_{sp}).



26984

A multi-year study of lower tropospheric aerosol variability and systematic relationships

J. P. Sherman et al.

Title Page

Abstract

Introduction

Conclusions

References

Tables

Figures

◀

▶

◀

▶

Back

Close

Full Screen / Esc

Printer-friendly Version

Interactive Discussion

The RH inside the nephelometer occasionally exceeded 40 % during the humid summer months (reaching as high as ~ 50 %), which can result in a small enhancement of light scattering above “dry” aerosol light scattering levels. To determine the magnitude of this effect, we applied scattering hygroscopic growth gamma fit parameters (Quinn et al., 2005) based on humidified light scattering and hemispheric backscattering measurements at APP and SGP (not included here) to the hourly-averaged light scattering and hemispheric backscattering values for hours when the nephelometer internal RH exceeded 40 %. For gamma values encompassing the 5th through 95th percentiles (i.e., basically the entire range of possible growth factors), the correction of light scattering and hemispheric backscattering from values at the elevated RH to values at RH = 40 % was less than 3–4 % and the uncertainty in applying static correction factors for sites with no humidified scattering measurements (BND, EGB) was similarly small. Based on these relatively small adjustments, hours with elevated nephelometer RH were retained and no RH corrections were applied to the scattering measurements for these hours.

3 Results and discussion

~~Regional and temporal variability of M_{10} and PM_{10} aerosol properties are presented in Sects. 3.1–3.3. The period of study is 2010–2013 and the measurements were made continuously or near-continuously at all four sites over the full period (Table 2). Section 3.1 presents annual cycles of monthly median aerosol properties at the four sites over this four year period. Differences in median values among the four sites for the entire period and for individual months were used to quantify regional variability. Comparisons of the annual cycles of aerosol properties at the long-term sites (SGP and BND) for the current period with those of the D&O2002 period and with the intervening years at SGP and BND provide a simple means for examining the influence of length of data set on the annual cycle of aerosol properties and how they have changed over time. Weekly and diurnal cycles of median aerosol properties over the four year period~~

A multi-year study of lower tropospheric aerosol variability and systematic relationships

J. P. Sherman et al.

Title Page

Abstract

Introduction

Conclusions

References

Tables

Figures

◀

▶

◀

▶

Back

Close

Full Screen / Esc

Printer-friendly Version

Interactive Discussion

are presented in Sects. 3.2 and 3.3 and similar comparisons with the long-term records are presented for SGP and BND. Median values were used to examine regional and temporal variability because medians are more robust in minimizing the effects of outliers than mean values and because medians facilitate comparisons with previous studies, including D&O2002. Temporal variability on each of the timescales was defined for the purposes of this study as the amplitude of the cycle of median values (difference between maximum and minimum values). Systematic relationships between aerosol properties and aerosol loading (using scattering at 550 nm as a proxy for loading) are presented in Sect. 3.4, both on an annual basis and for individual seasons.

All statistics presented in this paper are based on hourly-averaged, quality-assured σ_{sp} , σ_{bsp} , and σ_{ap} measurements, as outlined in Sect. 2.3 and references therein. The aerosol intensive properties were calculated using the formulas given in Table 1. For brevity, only aerosol properties at 550 nm are presented with the exception of scattering and absorption Ångström exponents. Scattering Ångström exponents were calculated based on the 450 and 700 nm scattering coefficients to provide a wavelength range closest to the range (440 to 870 nm) typically specified in studies based on AERONET data. Absorption Ångström exponents were calculated for both the 450/550 nm and 450/700 nm wavelength pairs so that the difference (i.e. higher value for 450/550 nm pair) could be used as an additional qualitative indicator of absorption by species other than black carbon (e.g., dust, brown carbon).

3.1 Annual cycle of aerosol extensive and intensive properties

Monthly median values of PM_{10} and PM_1 aerosol properties over the 2010–2013 period are shown for the four continental North American sites in Figs. 1 and 2 and are shown for three different time periods at the long-term sites (SGP and BND) in Figs. 3–5. Each trace of a given plot contains median values for individual months of the year over that period. For example, the “JAN” data point on the “1996–2013” trace of PM_{10} σ_{sp} for BND (Fig. 3) represents the median of all hourly-averaged BND PM_{10} σ_{sp} values (at 550 nm) during the January months in the period September 1996–December 2013.

The “ALL” point of each trace corresponds to the median value over that entire period.

should be noted that phrases such as “highly variable” and “similar values” used in this and subsequent sections have different meanings for different variables and studies. For example, aerosol DRF is particularly sensitive to single-scattering albedo. The critical ω_0 at which the surface forcing changes sign lies in the same range ($\sim 0.85\text{--}0.9$, dependent on underlying surface and aerosol vertical distribution) of ω_0 values often measured at the four sites (Hansen et al., 1997). As such, 5–10% seasonal variability in ω_0 would be much more climatically-significant than a similar change in scattering Ångström exponent.

3.1.1 Differences in median aerosol properties among the four sites

Differences in median aerosol properties among the sites for the entire four-year period (as seen from the “ALL” data points in Figs. 1 and 2) were used to quantify regional variability on an annual basis. PM_{10} and PM_1 σ_{sp} and σ_{ap} demonstrated the largest differences in median properties among sites. Median PM_{10} σ_{sp} was $\sim 25\%$ higher at BND than at SGP and APP. Median PM_1 σ_{sp} was also highest at BND, approximately a factor of 2 higher than EGB. These differences were largely influenced by cool- and cold-season months, as can be seen from the individual monthly median values (Fig. 1). Median PM_{10} and PM_1 σ_{ap} values were similar for BND and APP and median PM_1 σ_{ap} measured at both sites were nearly a factor of 2 higher than EGB. However, the fractional amounts of fine-mode aerosol scattering and absorption, indicated by R_{sp} and R_{ap} respectively, were clearly higher at APP than at either SGP or BND, both for the entire period and for all months of the year. PM_{10} scattering Ångström exponent (α_{sp}) serves as another indicator of the relative amount of fine-mode aerosol; α_{sp} was also highest for APP and was lowest for SGP (Fig. 1). The greater influence of super- $1\ \mu\text{m}$ particles to aerosol scattering and absorption at BND and SGP (relative to APP) is not surprising, given the larger agricultural influence (a source of dust production) in these regions of the US, while the forest density is much higher in the SE US. The forests in the SE US generate condensable organics (Goldstein et al.,

A multi-year study of lower tropospheric aerosol variability and systematic relationships

J. P. Sherman et al.

Title Page

Abstract

Introduction

Conclusions

References

Tables

Figures

◀

▶

◀

▶

Back

Close

Full Screen / Esc

Printer-friendly Version

Interactive Discussion

2009; Link et al., 2014), which enhance the PM_1 scattering values, especially during warm-season months. Land use patterns in the rural continental eastern US are more similar to APP than to SGP or BND, leading us to speculate that R_{sp} and R_{ap} values in the rural continental eastern US are probably closer to those of APP than of SGP and BND and that there is likely a west-to-east gradient in the relative influence of PM_1 to aerosol scattering and absorption.

The regional differences for the other aerosol intensive properties in Figs. 1 and 2 over the entire period were, in most cases, much less than the seasonal variability in monthly median values at the individual sites. This result indicates that seasonality must be considered when examining regional differences, at least for the four regions in this study. Similar results were obtained when using means and SDs over the entire study period (not shown), where the differences in most mean aerosol properties between the sites were substantially less than the SDs for the individual sites.

3.1.2 Seasonal variability as a function of region

The amplitude of the annual cycle in monthly median PM_{10} scattering coefficient (σ_{sp}) was much larger at APP than at SGP and BND, with monthly median σ_{sp} values increasing by a factor of ~ 3 from winter to summer (Fig. 1). EGB exhibited the largest seasonality in $PM_1 \sigma_{sp}$ and σ_{ap} , with comparable $PM_1 \sigma_{sp}$ seasonality at APP. Median PM_{10} and $PM_1 \sigma_{sp}$ were highest during July and/or August at all sites, followed by sharp decreases in September. All sites also exhibited absorption peaks in summer (typically highest in August) but the absorption peaks tended to be broader than the scattering peaks for all sites except EGB, where the autumn decreases in median $PM_1 \sigma_{sp}$ and σ_{ap} were similar (factor of ~ 3 to 4). In contrast, the autumn decreases in median PM_{10} and $PM_1 \sigma_{sp}$ at APP were twice as large as the autumn decreases in σ_{ap} . SGP and BND represented intermediate cases, with monthly median σ_{sp} decreasing ~ 1.5 times more than median σ_{ap} during autumn. The fact that the scattering and absorption seasonal cycles were different in terms of magnitude and broadness of peak suggests that there were different sources, sinks, and/or atmospheric processes affecting the

A multi-year study of lower tropospheric aerosol variability and systematic relationships

J. P. Sherman et al.

Title Page

Abstract

Introduction

Conclusions

References

Tables

Figures

◀

▶

◀

▶

Back

Close

Full Screen / Esc

Printer-friendly Version

Interactive Discussion

aerosol properties observed at each site. Summer-to-fall changes in σ_{sp} and σ_{ap} of similar magnitude at EGB indicate that primary aerosol sources were likely responsible for both the σ_{sp} and σ_{ap} seasonality at EGB while the much larger summer scattering enhancement at APP (relative to that of absorption) is consistent with particle growth dominating the large seasonality in σ_{sp} at APP, as discussed below. Particle growth and some seasonality in primary sources likely contributed to the seasonality in σ_{sp} and σ_{ap} at SGP and BND.

The large amplitudes of the annual PM_1 σ_{sp} and σ_{ap} cycles at EGB were primarily influenced by the seasonally-dependent frequency of south/southeasterly flow from the heavily-populated Toronto area and northeastern US (most frequent in spring and summer), for which higher mass concentrations of sulfates, organics, and black carbon (BC) are measured (Chan et al., 2010). Long-range transport of biogenic secondary organic aerosol (SOA) from boreal forests also influenced σ_{sp} at EGB during summer months for northwesterly flow (Chan et al., 2010). During fall and winter, the frequency of transport from the south is less and relatively cleaner northwesterly air masses prevail, resulting in lower scattering and absorption at EGB during these months.

The APP site is largely influenced by biogenic SOA during the warm season (Link et al., 2014) and the sharp autumn decrease in σ_{sp} (Fig. 1) is in agreement with seasonality in biogenic VOC precursor emissions in the SE US (Goldstein et al., 2009), along with reduced photochemistry. The annual cycle in σ_{sp} at APP is qualitatively similar to the seasonality in satellite-based measurements of SE US AOD reported by Goldstein et al. (2009), who showed that both the large seasonality in spatial AOD variability and the AOD dependence on temperature were consistent with SOA formed from biogenic VOC oxidation, mediated by anthropogenic precursor gases. Multi-year measurements reported by the IMPROVE network (Hand et al., 2011) showed that sulfates were the principal component of the surface-level $PM_{2.5}$ mass fraction for all months at IMPROVE sites in the Appalachian mountain region of the US (with mass fractions of ~ 0.6 during summer) but PM_1 chemical composition measurements made by an Aerodyne Aerosol Mass Spectrometer over two summers and one winter at APP revealed

A multi-year study of lower tropospheric aerosol variability and systematic relationships

J. P. Sherman et al.

Title Page

Abstract

Introduction

Conclusions

References

Tables

Figures



Back

Close

Full Screen / Esc

Printer-friendly Version

Interactive Discussion

that a majority of PM_1 non-refractory mass concentration is organic aerosol (Fig. S1 of the Supplement). The discrepancy could be due in part to the higher-elevation of the APP site. Based on aircraft measurements of aerosol composition made using an Aerodyne AMS, Kleinman et al. (2007) reported much higher organic mass fractions above the surface than measured by IMPROVE surface sites in the eastern US. A detailed analysis of the relative roles of sulfates and organics to the measured optical properties is beyond the scope of this paper and will form the topic of a future publication.

A majority of the warm-season PM_1 aerosol mass at SGP consists of low and highly-oxidized SOA (corresponding loosely to “fresher”, and “aged” organic aerosol, respectively) as reported by Fast et al. (2013), but the seasonal cycle in $PM_1 \sigma_{sp}$ at SGP during our study period was much weaker than that at APP or EGB. One hypothesis for this is that the crop vegetation that dominates at BND and SGP produces far less organic aerosols than the forests around APP and upstream EGB. In addition to a summer scattering peak, BND also exhibited a secondary PM_{10} and $PM_1 \sigma_{sp}$ peak during winter months. This was not accompanied by a secondary peak in σ_{ap} (leading to higher ω_0 during winter) and coincided with lower R_{sp} and R_{ap} values and higher α_{ap} (450/550 nm) values, indicating that larger, primarily scattering particles (including dust) influenced the winter scattering at BND.

Annual ω_0 cycle amplitudes were substantial at all sites, ranging from ~ 0.04 for PM_{10} at SGP (February vs. October) to ~ 0.13 for PM_1 at EGB (July vs. October) (Fig. 1). The annual PM_{10} and $PM_1 \omega_0$ cycle amplitudes at APP (~ 0.06) appear to be influenced almost entirely by the cycle in σ_{sp} , which in turn was likely influenced by biogenic SOA in the SE US during warm-season months. The large seasonal variability in $PM_1 \omega_0$ at EGB was due to the variety of PM_1 aerosol sources measured at the site, ranging from very clean air dominated by organics for north and westerly flow to episodic SE flow containing anthropogenically-influenced air masses with high levels of sulfates, organics, and BC (Chan et al., 2010). The low monthly median ω_0 values at EGB in September and October were more the result of very low aerosol loading

A multi-year study of lower tropospheric aerosol variability and systematic relationships

J. P. Sherman et al.

Title Page

Abstract

Introduction

Conclusions

References

Tables

Figures

◀

▶

◀

▶

Back

Close

Full Screen / Esc

Printer-friendly Version

Interactive Discussion

during those months (Fig. 1). Episodic agricultural burning occurs near EGB during fall months, but it is not expected to exert a major influence on median values. Aerosols measured at all sites exhibited a tendency toward lower ω_0 under clean air conditions for all seasons (as will be discussed in Sect. 3.4.1). Decreases in median ω_0 at SGP and BND for fall months, relative to summer months, were likely due to a combination of sharp autumn decreases in σ_{sp} , along with increased crop and grass fires and diesel emissions from combines and the transport of crops during the fall harvest. The winter increase in median ω_0 at BND resulted from the increase in larger, scattering particles during winter, as discussed above.

All sites demonstrated lower median b values for months and seasons when scattering was highest (most notably summer) and higher b values when scattering was lowest (autumn months). This relationship was most obvious at APP, where the summer-to-autumn increase in monthly median b was $\sim 35\%$, coinciding with a decrease in median σ_{sp} by a factor of ~ 2.5 . Summer-to-autumn differences in R_{sp} and PM_{10} α_{sp} at APP were much less than the differences in b , an effect that is also observed (to a much lesser degree) at SGP and BND.

Using Mie theory, Collaud Coen et al. (2007) conducted simulations to show that hemispheric backscatter fraction b at 550 nm is most sensitive to particles of diameter $D_p < 0.3 \mu\text{m}$ (their Fig. 7 and accompanying discussion). Schuster et al. (2006) combined simulations based on Mie theory with volume size distributions and AOD from AERONET to show that extinction Ångström exponent is relatively insensitive to fine mode effective radius for bi-modal aerosol size distributions and is a better indicator of volume fraction of fine mode aerosol. Smaller seasonal variability in α_{sp} and R_{sp} observed at APP, along with higher R_{sp} values (Figs. 1 and 2), is likely due to a higher and less variable fraction of fine-mode aerosol at APP. This will be discussed further in Sect. 3.4.4. The large summer-to-autumn difference in b (relative to α_{sp} and R_{sp}) at the four sites suggests that the major seasonal changes in the aerosol size distributions may lie in the lower end of the accumulation mode, with shifts toward larger particles in summer and smaller particles in fall. Photochemistry likely played a role in the ob-

A multi-year study of lower tropospheric aerosol variability and systematic relationships

J. P. Sherman et al.

Title Page

Abstract

Introduction

Conclusions

References

Tables

Figures

◀

▶

◀

▶

Back

Close

Full Screen / Esc

Printer-friendly Version

Interactive Discussion

served seasonal cycle of b , especially at APP (Fig. 1). Gas-to-particle conversion onto existing particles is most efficient for the 100–500 nm size range, since this is where most of the aerosol surface area typically lies (Seinfeld and Pandis, 1998). Reduced conversion in fall (when photochemistry and precursor levels are lower) would impact b more than α_{sp} and R_{sp} . Substantial fractions of summer SOA mass measured at APP and SGP consists highly-oxidized “aged” aerosol (Link et al., 2014; Fast et al., 2013).

Absorption Ångström exponents for both wavelength pairs (450/550 nm and 450/700 nm) were lowest during summer months for all three sites where spectral absorption measurements were available (Fig. 2). At APP, the monthly median α_{ap} values for both wavelength pairs were similar and well below 1 from May through September, which are the months of maximum biogenic VOC emissions and photochemistry in the SE US (Goldstein et al., 2009). Gyawali et al. (2009) performed simulations using Mie theory to show that α_{ap} values much less than 1 are possible (their Figs. 8 and 9) when absorbing particles are coated. Clarke et al. (2007) also reported a large number of α_{a} (470/660 nm) values clustered between 0.7–1.1 for pollution plumes during extensive flights over North America as part the of the INTEX/ICARTT experiment in summer 2004, although they did not hypothesize as to the source of the low α_{ap} values. Dust also contributed to July light absorption at SGP, as inferred from the lower monthly median R_{ap} (Fig. 2), particularly for the shorter wavelength pair (450/550 nm), where dust absorption is stronger. (Bergstrom et al., 2007). In the colder months, the combined values of α_{sp} and α_{ap} suggest a mix of absorbing aerosol such as black carbon (BC), along with brown carbon and/or dust (e.g., Cazorla et al., 2013) at SGP, BND, and APP. Lower values of R_{ap} during winter at BND suggest some contributions by dust to the absorption. The seasonal cycle of α_{ap} at BND and SGP were not as strong as at APP and the elevated winter monthly α_{ap} values at APP (in combination with low amounts of super-1 μm aerosol) are consistent with higher winter mass concentrations of SOA from biomass-burning (Link et al., 2014). Wood is a common residential heating fuel in the SE US (Zhang et al., 2010).

A multi-year study of lower tropospheric aerosol variability and systematic relationships

J. P. Sherman et al.

Title Page

Abstract

Introduction

Conclusions

References

Tables

Figures

◀

▶

◀

▶

Back


Close

Full Screen / Esc


Printer-friendly Version


Interactive Discussion



Median PM_{10} DRFE at EGB **was** the least negative of all sites for nearly all months, for reasons that are not obvious based solely on examination of the seasonality in median ω_0 and b (relative to that of the other sites). The PM_{10} and PM_{10} DRFE cycle amplitudes were generally only a few percent at all sites, with the exception of PM_{10} DRFE at EGB (and to a lesser degree BND) in early fall. The lack of seasonality (more so at APP and SGP) **was** due to the competing effects of changes in ω_0 and b at the sites for most months. Months with higher aerosol loading (e.g., summer months) coincided with larger, less absorbing particles (lower b and higher ω_0) at all sites and months with lower loading, such as most autumn months, **coincided with** smaller, more absorbing particles (higher b and lower ω_0). These results are in agreement with systematic relationships between b , ω_0 , and aerosol loading, presented in Sects. 3.4.1 and 3.4.2. Lower ω_0 likely contributed to less negative median PM_{10} DRFE at EGB and BND during autumn, in spite of higher b values. 

3.1.3 Influence of time period studied on annual cycles of aerosol properties at SGP and BND

Inter-annual variability studies require a longer dataset than currently available at EGB and APP, so this topic must wait for a future publication.  However, changes in the annual cycle of median aerosol properties and the influence of length of dataset can be studied in a simple manner for SGP and BND, which both have measurements beginning in the mid-1990s. Here we present a comparison of the annual cycles for three time periods: (1) the 1997–2000 period at SGP and 1996–2000 period at BND, coinciding with the period studied by D&O2002, (2) the 2010–2013 period of the current study; and (3) the long-term record (1997–2013 for SGP and 1996–2013 for BND) containing both studies and the period in between.

Median PM_{10} (PM_{10}) σ_{sp} for the 2010–2013 period **was only** $\sim 75\%$ (~ 65 to 70%) that of the D&O2002 period and $\sim 90\%$ ($\sim 85\%$) of the median value for the long-term period at both sites, as seen from the “ALL” values in Fig. 3. The decreases in PM_{10} and PM_{10} scattering at both sites for the current period **were**,  nearly constant

A multi-year study of lower tropospheric aerosol variability and systematic relationships

J. P. Sherman et al.

Title Page

Abstract

Introduction

Conclusions

References

Tables

Figures

◀

▶

◀

▶

Back

Close

Full Screen / Esc

Printer-friendly Version

Interactive Discussion

across the seasons, although differences between current period and D&O2002 for a few individual months (February at SGP and October at BND) were larger. The larger reductions in PM_{10} σ_{sp} led to lower R_{sp} values for all months of the current period, relative to D&O2002 (Fig. 3), although the seasonality in R_{sp} was similar for the three periods at both sites. The difference between current period and long-term R_{sp} was larger than the difference between long-term and D&O period R_{sp} for all months at both sites, indicating that much of the reduction in the influence of PM_{10} to total aerosol light scattering may have occurred during the current period. The substantial decrease in σ_{sp} at both sites is consistent with other studies (Collaud Coen et al., 2013; Hand et al., 2014) that presented large decreases in surface light scattering and light extinction in North America during the past decade.

Median PM_{10} and PM_{10} absorption (σ_{ap}) for the current period at BND was noticeably lower than for the 1996–2000 period (i.e. the D&O2002 period) for most months, with the most notable reductions occurring during April, September, and October (Fig. 3). These could be the result of decreases in the frequency of agricultural burning that impact the site during spring and fall (D&O2002). The slightly lower absorption measured by the CLAP, relative to the PSAP (Sect. 2.2), may also have played a minor role in the lower median absorption measured during the current period at BND. Median PM_{10} and PM_{10} ω_0 values at BND showed little change among the three periods for individual months, and for the periods as a whole. Both PM_{10} and PM_{10} absorption at SGP changed less than scattering among periods, resulting in lower median ω_0 values for most months of the current period, and for the period as a whole. This could suggest that the major sources of scattering and absorbing particles at BND are similar now to those in 1996–2000, while at SGP there may be new sources for absorbing particles (e.g., increased gas/oil production). Collaud Coen et al. (2013) did not analyze the SGP absorption data for trends, but they reported a decreasing trend in absorption at BND consistent with the observations here. While trend analyses of derived aerosol properties such as ω_0 would provide a valuable expansion of the analysis conducted by Collaud Coen et al. (2013), by providing information on processes affecting the aerosol

characteristics over time, such an analysis is beyond the scope of the current paper and will form the subject of a future publication.

In addition to the decreases in R_{sp} at SGP and BND for the current period, there were also differences in other indicators of aerosol size distribution between the periods. The median PM_1 b at both sites for the current period was $\sim 20\%$ higher than for the D&O2002 period and monthly median b was higher for all individual months of the current period. Median PM_{10} and PM_1 b values for the current period were also higher than the long-term period values for all months at BND and most months at SGP. This indicates shifts in the lower size region of the accumulation mode (e.g., particles with $D_p \sim 0.1\text{--}0.3\ \mu\text{m}$) toward smaller particles over all seasons at both sites, based on similar reasoning to that of the previous section. Scattering Angstrom exponent (α_{sp}) at SGP was lower by small amounts ($\sim 0.1\text{--}0.3$) for all months of the current period, relative to D&O2002 (D&O2002 had very similar annual cycle to long-term period), which is consistent with the observed decrease in R_{sp} and suggests increasing relative contributions to scattering by coarse mode particles at SGP. In contrast, the amplitude of the annual cycle of median α_{sp} at BND has changed very little, despite the decrease in R_{sp} at that site. The likely cause is different shifts in the size distributions at the two sites. One possible source for reduction in PM_1 scattering at BND could be reduced emissions of anthropogenic precursor gases (mainly SO_2) by power plants in the region. BND is located in one of the US regions with highest sulfate burdens during the D&O2002 period (Koloutsou-Vakakis et al., 2001). Annual US SO_2 emissions from power plants decreased at a rate of $\sim 6\% \text{ year}^{-1}$ from 2001–2010, corresponding to the period in between to the D&O2002 study to the beginning of our study, with similar reductions in sulfate concentrations at rural US sites (Hand et al., 2012). Reduced gas-to-particle conversion resulting from reductions in gas-phase precursor emissions would shift the lower size region of the accumulation mode toward smaller particles and thereby reduce PM_1 scattering, while leaving the larger region of the size distribution less affected. The shift in size distribution at SGP also appears to be toward smaller aerosols in the lower size region of accumulation mode (as suggested by larger b) but

A multi-year study of lower tropospheric aerosol variability and systematic relationships

J. P. Sherman et al.

Title Page

Abstract

Introduction

Conclusions

References

Tables

Figures

◀

▶

◀

▶

Back

Close

Full Screen / Esc

Printer-friendly Version

Interactive Discussion



A multi-year study of lower tropospheric aerosol variability and systematic relationships

J. P. Sherman et al.

Title Page

Abstract

Introduction

Conclusions

References

Tables

Figures

◀

▶

◀

▶

Back

Close

Full Screen / Esc

Printer-friendly Version

Interactive Discussion

with a larger relative contribution from coarse-mode aerosols (as evidenced by smaller R_{sp} and α_{sp}). The source for this shift in size distribution could be less gas-to-particle conversion, along with a new source of large particle aerosol (fracking or oil production in the region or else dust associated with more pronounced droughts during recent years. The annual cycle in median PM_{10} and PM_1 absorption Ångström exponent (α_{ap}) changed very little at BND and SGP, although α_{ap} measurements at these sites were only initiated in the mid-2000s. Likewise, the changes in the annual cycle of PM_{10} and PM_1 DRFE were small at both sites, although small decreases (more negative values) were observed at BND for all months.

3.2 Weekly cycle of aerosol extensive and intensive properties

Hourly-averaged aerosol properties were binned by day of week over the 2010–2013 period to examine their weekly cycles and to compare the weekly cycles across periods at the long-term sites (SGP and BND), in a similar manner to the annual cycle analysis of Sect. 3.1. Day of week variability in aerosol properties can be used as a tool for distinguishing anthropogenic from natural aerosol sources, since natural sources would not be expected to have aerosol properties that vary on weekly scales (Murphy et al., 2008). Due to the dependence of most aerosol properties on season (Sect. 3.1.2), the weekly cycles in the current period were examined over full years and also for individual seasons.

3.2.1 Day of week variability as a function of region

There was small day of week variability, median scattering and all intensive properties for all sites over the 2010–2013 period, with larger variability in absorption. The amplitudes of the weekly PM_{10} and PM_1 σ_{sp} cycles were $\sim 10\%$ or less at all sites, when examined over full years (Fig. S2 in the Supplement to this paper). The weekly σ_{sp} cycle amplitudes were also 10% or less for all individual seasons at EGB and for all seasons except autumn at BND, when it was roughly 30% , with maxima on Tuesday

A multi-year study of lower tropospheric aerosol variability and systematic relationships

J. P. Sherman et al.

Title Page

Abstract

Introduction

Conclusions

References

Tables

Figures

◀

▶

◀

▶

Back

Close

Full Screen / Esc

Printer-friendly Version

Interactive Discussion

and Wednesday. It reached 20 % during fall and winter at SGP (with a mid-week peak during autumn and no real pattern during winter). Median PM_{10} and PM_1 σ_{sp} during summer at APP was constant for Sunday–Tuesday, followed by a ~ 25 % step increase on Wednesday, after which it decreased at a very slow rate through Saturday. A similar but less pronounced weekly σ_{sp} cycle **was** present in spring at APP and absorption followed a similar weekly cycle at APP for all seasons except winter, as discussed below. Link et al. (2014) analyzed the relative abundances of light hydrocarbons to alkyl nitrates measured at APP, and concluded from alkyl nitrate formation kinetics that most of the air masses measured during the sampling period had undergone one to three days of photochemical processing. The step-like increase in σ_{sp} on Wednesday and higher values through Saturday is thus consistent with regional emissions during Monday–Friday. The fact that this occurs primarily during the warm season could be due to convectionally-driven increases in regional transport.

The amplitude of the weekly cycle in median b and ω_0 for both size cuts was ~ 0.01 or less at all sites for all seasons, with the exception of summer and fall PM_1 ω_0 at EGB, where it was 0.02 in summer (lowest on Friday) and 0.03 in fall (lowest on Tuesday). The amplitudes of the aerosol scattering and absorption Ångström exponent (α_{sp} and α_{ap}) cycles were on the order of 0.1 or less for all seasons at all sites. Day of week median DRFE fluctuated by $\sim 1 W m^{-2}$ or less except for PM_1 DRFE at EGB, which had variability of between 2 and $3 W m^{-2}$ for all seasons, with most negative values on Sundays and least negative on Tuesday and Wednesdays (Fridays in summer). Day of week median R_{sp} and R_{ap} variability was negligible for all seasons at APP (~ 0.01), small at BND (~ 0.03), and slightly larger (~ 0.05) at SGP. The minimum median R_{sp} at SGP occurred on Tuesday for all seasons, **possibly** due to some weekly pattern in agricultural activity near the site.

The amplitudes of the weekly cycles in median σ_{ap} over full years (the “All Months” plot in Fig. 6) were higher (~ 15 –30 %) than those in σ_{sp} at all sites and were highest for APP and EGB. Median absorption at all sites was lowest on Sunday and/or Monday when studied over full years. The apparently lower Sunday and Monday σ_{ap} at SGP

A multi-year study of lower tropospheric aerosol variability and systematic relationships

J. P. Sherman et al.

Title Page

Abstract

Introduction

Conclusions

References

Tables

Figures

◀

▶

◀

▶

Back

Close

Full Screen / Esc

Printer-friendly Version

Interactive Discussion

(Fig. 6) was possibly an artifact due to the lack of PSAP filter changes on weekends at the site; weekend days with high absorption would lead to overloaded filters and under-representation in the database, while weekend days with low absorption would be well-represented. Figure 6 also shows the weekly cycle of median σ_{ap} for individual seasons, which reveal several features not seen on the annual plot, namely (1) the absorption minima on Sunday and Monday was observed at APP (and possibly SGP) over all individual seasons but was not observed at BND during fall and winter or at EGB during spring, (2) weekly cycle amplitude in median σ_{ap} was often significantly larger (up to ~ 60–70 % for SGP and EGB) for individual seasons (Fig. 6), (3) the weekly absorption cycle at APP followed the same general progression for all seasons except winter, with steady increases leading to a broad maximum on Wednesday–Friday, followed by a weekend decrease. The cycle amplitude was largest in summer, similar to that of scattering at APP. The discussions above related to summer weekly scattering cycle at APP may also apply for the absorption cycle at APP, (4) BND exhibits strong day of week σ_{ap} variability during all seasons except winter (when convection and transport is weakest) but the peak day varies with season. Median σ_{ap} at BND exhibits a steady increase throughout the week during summer, reaching a peak on Friday, while in autumn the absorption peaks on Tuesday and decreases through the remainder of the week. The summer pattern at BND could be due to convectionally-driven increases in regional transport, with weekly patterns in agricultural and transportation activities the likely source for large cycles during the other seasons. Each of these features illustrates the need to quantify day of week absorption variability on a seasonal basis.

Murphy et al. (2008) utilized speciated mass concentration data from IMPROVE monitoring sites in the US over the years 2000–2006 to study day of week variability in aerosol composition. Results from their study included black carbon and soil dust concentration minima on Sunday and Monday, but minimal weekly cycling of organic carbon or sulfate. One of their conclusions was that diesel emissions likely play a large role in black carbon aerosols over the entire US and that much of the soil dust in the US was likely anthropogenic. They also found that aerosol light absorption at SGP (1999–

A multi-year study of lower tropospheric aerosol variability and systematic relationships

J. P. Sherman et al.

Title Page

Abstract

Introduction

Conclusions

References

Tables

Figures



Back

Close

Full Screen / Esc

Printer-friendly Version

Interactive Discussion



2005) and BND (1999–2002) followed a similar weekly cycle as black carbon and soil dust, while scattering variability on this timescale was negligible. The general lack of weekly scattering variability for all sites in our study and for SGP and BND in other studies (Murphy et al., 2008; Sheridan et al., 2001) could be related to the absence of weekly cycles in organic carbon or sulfate concentrations (Murphy et al., 2008), since these represent the primary sources of PM_{10} scattering particles at all sites in our study (Fast et al., 2013; Koloutsou-Vakakis et al., 2001; Chan et al., 2010; Fig. S1 of Supplement to this paper). The larger weekly absorption cycle at all sites (relative to scattering) suggests that the some of the sources for scattering and absorbing aerosols were likely different. The Sunday and Monday σ_{ap} minima present in nearly all cases of our study and similar weekly variability in σ_{ap} to that noted by Murphy for BC concentrations in the US (up to $\sim 20\%$) could indicate that diesel emissions played a large role in the absorption measured at each site. The weekly pattern in σ_{ap} at APP over all seasons except winter indicates that the emissions controlling the weekly absorption cycle were likely regional in nature, as discussed above. This could also be the case for the other **sites, although it** is not as apparent from Fig. 6.

3.2.2 Influence of time period studied on weekly cycles of aerosol properties at SGP and BND

The weekly cycle in median PM_{10} and PM_{10} aerosol intensive properties exhibited the same lack of variability for the D&O2002 and the long-term periods at SGP and BND as for the current period. The only notable difference in the weekly cycle of aerosol properties between periods was the elevated median PM_{10} and PM_{10} σ_{sp} at BND (and to a lesser degree, SGP) on weekends during the D&O2002 period. Amplitudes of the weekly cycle of median PM_{10} and PM_{10} σ_{sp} at BND were only $\sim 10\%$ for full years during the current period (with a broad peak between Tuesday and Thursday) and were even less for the long-term period. However, there was a weekend peak in median PM_{10} and PM_{10} σ_{sp} at BND during the D&O2002 period, with values $\sim 25\%$ higher than for the Wednesday/Thursday minima. A similar weekend peak was observed at SGP during

the D&O2002 period, although it was less pronounced ($\sim 15\%$ above the Thursday σ_{sp} minima) than at BND. The median R_{sp} during that period was ~ 0.85 to 0.90 for weekend days at both sites during the **D&O** time period so the enhanced weekend σ_{sp} was likely not dust but rather some anthropogenic PM_1 source that no longer exerts a major influence on σ_{sp} , since the weekend σ_{sp} enhancement is not seen in either the long-term or current period weekly cycle at either site.

3.3 Diurnal cycle of aerosol extensive and intensive properties

Hourly-averaged aerosol properties were binned by hour of day over the 2010–2013 period to examine their diurnal cycles and also to compare the diurnal cycles across periods at the long-term sites (SGP and BND), in a similar manner to the weekly cycle analysis of Sect. 3.2. Diurnal variability can be used to infer the influence of local sources and boundary layer height on the dried near-surface aerosol properties, ~~among other things~~. A purely boundary layer effect at the four non-urban sites would likely give rise to a single broad afternoon minima and late evening to early morning maxima in the diurnal σ_{sp} and σ_{ap} cycles due to the diurnal evolution of the mixed layer height, which is influenced by solar heating. **A** local traffic influence would result in a diurnal σ_{ap} cycle nearly in phase with local traffic patterns, with peaks typically occurring during early morning and late afternoon to early evening. A local traffic influence would also result in a larger diurnal cycle in σ_{ap} than σ_{sp} for mid-visible wavelengths, due to the higher BC fractions in fresh diesel emissions (US EPA, 2002). Regional traffic sources such as steady interstate traffic can be difficult to separate from boundary layer effects through diurnal cycle timing alone but may be separable based on the relative cycle amplitudes of absorption and scattering. Due to the dependence of most aerosol properties on season (Sect. 3.1.2), the diurnal cycles for the current period **were** examined over the full year and also for individual seasons.

A multi-year study of lower tropospheric aerosol variability and systematic relationships

J. P. Sherman et al.

Title Page

Abstract

Introduction

Conclusions

References

Tables

Figures

◀

▶

◀

▶

Back

Close

Full Screen / Esc

Printer-friendly Version

Interactive Discussion



3.3.1 Diurnal variability as a function of region

Similar to the weekly cycles, the scattering diurnal cycle amplitudes **were** modest. When studied over full years, the amplitude of the PM_{10} σ_{sp} diurnal cycle was $\sim 10\%$ at APP and marginally higher at BND and SGP, with slightly less diurnal variability in median PM_1 σ_{sp} at all sites (Fig. 7). Broad mid to late-afternoon PM_{10} and PM_1 σ_{sp} minima were observed at SGB, BND, and (PM_1 only) EGB, consistent with some influence of boundary layer height on the diurnal σ_{sp} cycles. A smaller, narrow early afternoon σ_{sp} minima was observed near 13:00 Local Standard Time (LST) at APP, likely due to a combination of less mid-day local traffic and dilution due to elevated boundary layer heights, the latter of which are derived from vertical aerosol backscatter profiles measured by a micro-pulsed lidar at APP (not shown). The amplitudes of the diurnal cycles in PM_{10} and PM_1 σ_{ap} **were** larger than those of σ_{sp} at all sites; roughly 30–35% at SGP and BND and ~ 15 –20% at APP and (PM_1 only) EGB (Fig. 7). The larger cycles in σ_{ap} indicate some local and/or regional traffic influence at all sites.

The impact of local traffic on the diurnal σ_{ap} cycle was most notable at APP and EGB, as seen by relatively narrow morning peaks during hours of maximum traffic (07:00–09:00 LST). The afternoon σ_{ap} minima at APP was also narrower than that of the other sites and occurred earlier in the afternoon (near 12:00 LST), similar to the narrow mid-day σ_{sp} minima. The APP site is not located near any major highways but is located 1 to 3 km from local commuter traffic sources during weekday mornings and late afternoons. EGB is a remote site but is located approximately 15 km from a major interstate highway and **also** experiences some influence from the nearby city Barrie when the wind comes from that direction. The highway experiences heavy commuter traffic during early morning and late afternoon.

SGP and BND demonstrated only a single broad afternoon σ_{ap} minima and broad evening to early morning peak (Fig. 7), suggesting a greater influence of boundary layer height evolution to the σ_{ap} diurnal cycles at these sites, along with possibly regional traffic. Both sites experience infrequent local traffic but are situated ~ 8 to 15 km to

A multi-year study of lower tropospheric aerosol variability and systematic relationships

J. P. Sherman et al.

Title Page

Abstract

Introduction

Conclusions

References

Tables

Figures

◀

▶

◀

▶

Back

Close

Full Screen / Esc

Printer-friendly Version

Interactive Discussion



A multi-year study of lower tropospheric aerosol variability and systematic relationships

J. P. Sherman et al.

Title Page

Abstract

Introduction

Conclusions

References

Tables

Figures

◀

▶

◀

▶

Back

Close

Full Screen / Esc

Printer-friendly Version

Interactive Discussion

the west (and predominantly upwind) of major interstate highways (I-35 for SGP and I-57 for BND) that experience truck traffic over all hours, with some increase in traffic volume during early morning. Thus regional traffic may have contributed to the diurnal cycles in σ_{ap} (and to a lesser extent σ_{sp}) at SGP and BND, in contrast to the commuter influence at APP and the mixture of regional and commuter traffic influence at EGB.

Diurnal variability of aerosol intensive properties was minimal at all sites when studied over full annual cycles, with a few minor exceptions: (1) a small early morning decrease (~ 0.05) in R_{ap} at SGP, (2) small (0.2) decreases in α_{ap} (450/550 nm) during the day at BND, SGP, and a smaller amount at APP during the day, possibly indicative of a greater relative influence of BC to the absorption.

The diurnal variability of σ_{ap} was much larger than the day of week variability for all individual seasons at SGP and BND, winter and spring at APP, and summer and fall at EGB (Fig. 8). The amplitude of the diurnal PM_{10} and PM_1 σ_{ap} cycles at APP were ~ 15 – 20 % for all seasons and were ~ 40 % for all seasons at SGP. Features similar to those over full annual cycles were present for each individual season at APP and SGP, namely the influence of morning commuter traffic at APP and the broad single peak and minima suggesting boundary layer influence and possibly regional traffic at SGP. In contrast, the amplitude of the diurnal σ_{ap} cycles at BND and EGB varied substantially with season and was largest in summer and fall at both sites. The seasonally-dependent diurnal σ_{ap} cycle amplitudes at BND (Fig. 8), along with the widths of the single broad daytime minima and night-time maxima that coincided with the diurnal cycle of solar insolation for all seasons, seem to implicate boundary layer dynamics for at least part of the large diurnal σ_{ap} cycle. The large summer and fall PM_1 σ_{ap} diurnal cycles at EGB showed some influence from boundary layer height (e.g., the broad late morning to afternoon minima and the late evening maxima), in addition to the local traffic influence observed during autumn mornings. However, the summer and fall σ_{ap} diurnal cycles at EGB also include a peak within two hours of local midnight, followed by sharp decreases until $\sim 05:00$ LST. This is not consistent with known traffic patterns near the site nor with a boundary layer height influence. One

other interesting feature in the σ_{ap} cycles is that the time of morning peak at APP and EGB lags the time of the peak at BND and SGP by roughly two hours for all seasons. Possible explanations include (1) differences in morning boundary layer heights over cropland and forested areas; and (2) differences in traffic sources (as discussed in the previous paragraphs).

The diurnal cycle amplitudes of most aerosol intensive properties were small for all seasons, as illustrated in Figs. S3–S6 of the Supplement. The amplitudes of the PM_{10} and PM_1 b cycles were ~ 0.01 or less at all sites for all seasons and the α_{sp} cycle amplitudes were ~ 0.1 or less for all sites and seasons, with exception of summer at SGP (when it was 0.3, with minima near hour 18:00 LST). Diurnal variability of R_{sp} was negligible for APP and was ~ 0.03 for SGP and BND for all seasons except summer at BND, where it was ~ 0.05 (with minima near 06:00 LST). These small cycle amplitudes are comparable to those for the weekly cycles and indicate that median values of indicators of aerosol size distributions at all sites exhibited little variability on shorter time scales (diurnal and day of week).

The amplitude of the diurnal R_{ap} cycle **was only** ~ 0.02 for all seasons at BND and APP but **was** larger at SGP, with morning minima in R_{ap} at SGP coinciding with hours of peak traffic (07:00 to 10:00 LST). The morning minima in R_{ap} at SGP are most obvious in summer, with values ~ 0.10 less than the daily maxima. In addition, the hour of minimum R_{ap} for all seasons coincided with times of low absorption, signifying lower levels of absorbing PM_1 during this time as opposed to elevated levels of absorbing mineral dust generated by agricultural activities or traffic near the site.

Diurnal variability in median PM_{10} and PM_1 ω_0 **was** slightly larger than day of week variability but much less than seasonal variability at all sites, with cycle amplitudes of ~ 0.01 to 0.02 for most sites and seasons. There **were** a few exceptions. The PM_1 ω_0 diurnal cycle amplitude at SGP was ~ 0.03 during summer and ~ 0.04 in **fall, with** broad afternoon maxima and late evening to early morning minima for both seasons, influenced by the σ_{ap} diurnal cycle. Diurnal variability in PM_1 ω_0 at EGB **was** ~ 0.04 during summer (with the same broad afternoon peak and late evening to early morn-

A multi-year study of lower tropospheric aerosol variability and systematic relationships

J. P. Sherman et al.

Title Page

Abstract

Introduction

Conclusions

References

Tables

Figures

◀

▶

◀

▶

Back

Close

Full Screen / Esc

Printer-friendly Version

Interactive Discussion



A multi-year study of lower tropospheric aerosol variability and systematic relationships

J. P. Sherman et al.

Title Page

Abstract

Introduction

Conclusions

References

Tables

Figures

◀

▶

◀

▶

Back

Close

Full Screen / Esc

Printer-friendly Version

Interactive Discussion

ing minima as SGP) and was ~ 0.05 in fall (with sharp minima near 07:00 LST and 19:00 LST likely due to local traffic). The variability in ω_0 at EGB led to diurnal variability in DRFE of 3 W m^{-2} in summer and 4 W m^{-2} in fall. Diurnal variability in median DRFE was typically 1 to 2 W m^{-2} for all other sites and seasons. Diurnal variability in median α_{ap} (450/700 nm) was negligible for SGP, BND, and APP for all individual seasons but there were small cycles in α_{ap} (450/550 nm) of ~ 0.2 at BND during all seasons, SGP during winter and spring, and APP during summer, with smaller cycles during the other seasons. In all cases, the highest median α_{ap} (450/550 nm) values occurred over the early evening hours until near sunrise, with minima during early to mid-morning at SGP and BND and afternoon at APP. Increases in absorption in the blue-violet portion of visible spectrum are indicative of non-BC sources (dust or brown carbon). No consistent patterns in the diurnal cycles in median R_{sp} and R_{ap} were present to indicate the influence of dust to the small cycle of α_{ap} (450/550 nm) and biomass burning influences the three sites to various degrees during the year so it is possible that brown carbon produced by wood burning could be responsible for the small diurnal cycles in α_{ap} (450/550 nm).

3.3.2 Influence of time period studied on diurnal cycles of aerosol properties at SGP and BND

Median PM_{10} and PM_1 σ_{sp} and σ_{ap} at BND were lowest for all hours of the most recent (2010–2013) period, as was the diurnal cycle amplitude of each parameter (Fig. 7). Median σ_{sp} at SGP was also lowest for this period over all hours and the diurnal variability was perhaps slightly less than for the other two periods (1997–2000 and 1997–2013). The amplitude of the diurnal cycle in median σ_{ap} at SGP was slightly larger for the most recent period, with a more pronounced absorption dip from late morning through early evening. This gave rise to a larger cycle amplitude in median ω_0 at SGP for the most recent period (~ 0.03 for PM_1 and 0.02 for PM_{10}) than for either the D&O2002 or long-term periods (~ 0.01 for both periods). In addition there was a slightly larger DRFE variability ($\sim 2 \text{ W m}^{-2}$) for the most recent period. Diurnal cycle amplitude in

median ω_0 at BND **was** small (~ 0.01) for all three periods, as was that of DRFE variability ($\sim 1 \text{ W m}^{-2}$). The results for all indicators of aerosol size were similar to those in Sect. 3.1.3, with highest median b and lowest median R_{sp} occurring during the 2010–2013 period for all hours at both sites, along with negligible inter-period changes in median α_{sp} for all hours at BND. Median values of α_{sp} at SGP were slightly lower (by ~ 0.1 – 0.2) for all hours of the most recent period. There was small diurnal variability for each of these properties over any period at either site, signifying that the aerosol size distributions likely exhibited little diurnal variability over any of the periods.

3.4 Systematic relationships among aerosol properties

Systematic relationships among aerosol intensive properties and aerosol loading **were** explored at the four North American sites for the 2010–2013 period, both on an annual basis and broken down by season (Figs. 9–12). D&O2002 suggested systematic relationships would be useful for constraining model parameterization of aerosol optical properties and for reducing uncertainties in satellite-based retrievals of aerosol optical depth, which make assumptions regarding aerosol size distributions and ω_0 (Levy et al., 2010). Systematic relationships can also provide information regarding aerosol source types and processes. Relationships between mean aerosol intensive properties and aerosol loading, represented by aerosol light scattering σ_{sp} at 550 nm, **were** investigated for each season at each site by separating hourly-averaged σ_{sp} values into 10 M m^{-1} bins and then calculating the mean aerosol optical properties for each σ_{sp} bin. The x values for the data points on each plot correspond to the bin center. The relatively high ω_0 values at all sites justifies the use of σ_{sp} as a proxy for loading. Mean values were used to facilitate comparisons with D&O2002. Similar to the methods in Andrews et al. (2011), the standard error (SE = **SD**/square root of number of sample points) of the aerosol property was calculated for each σ_{sp} bin, and the bin was only included on the systematic variability plot if the standard error was less than 5 % of the typical y axis parameter value. These standard error thresholds were set at the follow-

A multi-year study of lower tropospheric aerosol variability and systematic relationships

J. P. Sherman et al.

Title Page

Abstract

Introduction

Conclusions

References

Tables

Figures

◀

▶

◀

▶

Back

Close

Full Screen / Esc

Printer-friendly Version

Interactive Discussion



ing: ω_0 : 0.05, b : 0.005, DRFE: 1, α_{ap} : 0.05, α_{sp} : 0.1, R_{sp} : 0.037. For brevity, only the PM_{10} curves are shown for SGP, BND, and APP, along with PM_1 curves for EGB. The corresponding PM_1 curves at SGP, BND, and APP look similar to the PM_{10} curves for these sites. Relationships between a few select intensive properties are also included to provide more insight into aerosol sources and/or processes influencing the properties measured at the sites. The same 5% SE thresholds for the dependent variable were also applied to these plots.

3.4.1 Single scattering albedo and backscatter fraction vs. scattering coefficient

Single scattering albedo increased and hemispheric backscatter fraction decreased with increasing aerosol loading for most sites and seasons (Fig. 9), indicative of greater influences by smaller, darker particles under low loading conditions and by larger, brighter particles under high loading conditions. Lower ω_0 and higher b values for low aerosol loading have been reported in other studies (D&O2002, Andrews et al., 2011) and are consistent with preferential removal of large, scattering particles by cloud scavenging and/or deposition. They can also be the result of new particle formation with growth by condensation and/or coagulation to optically-active sizes (Andrews et al., 2011).

The relative contributions of scattering and absorption to light extinction remained nearly constant for σ_{sp} greater than $45 \pm 10 \text{ M m}^{-1}$ for all seasons except spring at EGB, suggesting that primary sources of scattering and absorbing aerosol were responsible for the high loading events at EGB for most seasons- likely pollution transport from the south/southeast. Primary aerosol influence was also seen over most of the σ_{sp} range during spring at SGP and winter at APP. These are seasons with larger biomass burning influence in the two regions, namely field and crop burning during spring at SGP (Kohler et al., 2011) and regional wood-burning in the SE US during colder months (Zhang et al., 2010).

A multi-year study of lower tropospheric aerosol variability and systematic relationships

J. P. Sherman et al.

Title Page

Abstract

Introduction

Conclusions

References

Tables

Figures

◀

▶

◀

▶

Back

Close

Full Screen / Esc

Printer-friendly Version

Interactive Discussion

Regions of the ω_0 vs. σ_{sp} curves with positive slopes indicate different sources of scattering and absorbing aerosol, with particle growth often leading to the larger relative contributions by scattering. Single-scattering albedo increased with σ_{sp} for all seasons at BND and for all but the above-mentioned seasons at SGP, EGB, and APP. It also increased up to $\sim 45 \text{ M m}^{-1}$ for all seasons at EGB. The larger, more reflective particles with increased loading at APP during summer (and to a lesser degree spring and fall) may be due to condensation of organic and inorganic matter onto existing particles, as discussed in Sects. 3.1.2 and 3.4.7. Most of the spring and fall high-loading events at APP occur close to summer when emissions and photochemistry are significant. The SGP ω_0 vs. σ_{sp} curves for most seasons demonstrate a positive slope over a majority of the range of observed loading values, followed by some degree of flattening at high ω_0 values for $\sigma_{sp} \geq 55 \text{ M m}^{-1}$. Similar characteristics are present in the winter curve at BND. Primary sources such as wind-blown dust could have contributed to the large, highly reflective particles influencing high-loading summer and winter events at SGP and winter events at BND, as mean R_{sp} decreased sharply with increasing σ_{sp} during these seasons (Fig. 11).

3.4.2 Direct radiative forcing efficiency vs. scattering coefficient

Unlike ω_0 and b , the DRFE vs. σ_{sp} relationship did not follow a distinct trend and was unique to each site (Fig. 9). On an annual basis, DRFE for SGP became slightly less negative with increasing σ_{sp} , similar to that presented in D&O2002. Although the shapes of the SGP curves varied with season, the DRFE values for all but lowest and highest loading were within 2–3% of the annual curve. Similarly, the annual DRFE for APP became slightly less negative with increasing σ_{sp} over a large majority of the curve, with slightly larger slopes for the winter and summer curves and DRFE values lying within 4–5% of the annual curve for all but the lowest loading (where aerosol forcing is less important) over all seasons. The overall small increase in DRFE with increasing σ_{sp} indicates that, in terms of DRFE, the b vs. σ_{sp} relationship was slightly more important than the ω_0 vs. σ_{sp} relationship for most seasons and loading levels at

A multi-year study of lower tropospheric aerosol variability and systematic relationships

J. P. Sherman et al.

Title Page

Abstract

Introduction

Conclusions

References

Tables

Figures

◀

▶

◀

▶

Back

Close

Full Screen / Esc

Printer-friendly Version

Interactive Discussion

SGP and APP; additionally the small slope helps to explain the lack of seasonal DRFE variability at these sites. The annual DRFE vs. σ_{sp} curve at BND is flat to within $\sim 2\%$ for $\sigma_{sp} < 100 \text{ M m}^{-1}$, which encompasses all but the highest loading events. However, inspection of the seasonal curves reveals that the slope changes sign with season over much of the curve and that (at a given loading level) the differences from the annual curve can approach 7–8% for winter (when DRFE is more negative due to higher ω_0) and fall (when DRFE is less negative, due to lower ω_0). The largest seasonal differences between the curves occur in the range of σ_{sp} values typical of monthly medians at BND (25–50 M m^{-1}), consistent with slightly larger seasonal DRFE variability at BND, relative to that at SGP and APP.

The DRFE vs. σ_{sp} relationship varied the most between seasons for PM_{10} at EGB. Local maxima in mean DRFE occurred for $\sigma_{sp} < 20 \text{ M m}^{-1}$, except during summer, when the maxima occurred near 35 M m^{-1} , after which DRFE became more negative with increasing σ_{sp} until reaching a minimum and then increasing again for very high loading. Differences between the curves for individual seasons and the annual curve reached $\sim 10\%$ for several loading levels, indicating that the annual curve is a poorer representation of the relationship between DRFE and σ_{sp} at EGB. In addition, the magnitude and sign of the slopes changed between seasons for typical monthly median PM_{10} σ_{sp} levels at EGB ($\sim 10\text{--}30 \text{ M m}^{-1}$), consistent with the larger seasonal PM_{10} DRFE variability at EGB (Fig. 2). It should again be noted that the higher DRFE variability at EGB was not due to comparing PM_{10} for EGB with PM_{10} for the other sites, a result that can also be seen in the PM_{10} DRFE seasonal variability plots (Fig. 2).

3.4.3 Backscatter fraction vs. single-scattering albedo

Mean hemispheric backscatter fraction b , calculated for ω_0 bin sizes of 0.05, is shown for the four sites in Fig. 10. Systematic relationships between ω_0 and other aerosol intensive properties can provide information about aerosol composition and size distributions (Andrews et al., 2011). The b vs. ω_0 curves for all sites and seasons exhibited

negative slopes for the majority of the ω_0 range (0.80–1.0) typically measured at the sites, indicative of a less absorbing aerosol with increasing particle size. Similar relationships have been observed in studies involving high-elevation sites (Andrews et al., 2011) and for surface and aircraft-based measurements above SGP (Andrews et al., 2006). Andrews (2006) hypothesized that the relationship could be the results of preferential scavenging of large, primarily scattering aerosol but it could also be indicative of particle growth. The curves are also consistent with the b vs. σ_{sp} and ω_0 vs. σ_{sp} curves (Fig. 9). The points on each seasonal curve are within ~ 0.01 of the annual curve for all sites-indicating that a single annual curve is sufficient for the four sites in this study.

3.4.4 Sub-1 μm scattering fraction vs. scattering Ångström exponent

Mean R_{sp} increased proportionally with α_{sp} for all seasons at SGP, BND, and APP, though the slopes were different in winter and summer at low α_{sp} (Fig. 11). D&O2002 reported similar results for SGP and BND when studied on an annual basis. The fact that the R_{sp} vs. α_{sp} relationship is much stronger than either of their relationships with σ_{sp} (Fig. 11) suggests that α_{sp} is a better indicator of the relative magnitudes of coarse and fine mode aerosols than an indicator of average particle size. Schuster et al. (2006) applied Mie theory and spectral AOD and size distributions from AERONET sites to demonstrate an inverse relationship between extinction Ångström exponent and fine-mode effective radius for a purely mono-modal aerosol size distribution. They also demonstrated that increasing the fraction of coarse-mode aerosol in a bi-modal size distribution dampens the sensitivity of Ångström exponent to fine-mode effective radius, although it does provide some information as to the fine-mode aerosol volume fraction. Based on the range of R_{sp} values measured at SGP, BND, and APP, the aerosol size distributions were on average bi-modal (with higher coarse-mode fractions at SGP and BND than at APP) and care must be exercised when using α_{sp} to infer average particle size or aerosol type. The R_{sp} vs. α_{sp} relationship (Fig. 11) is consistent with simultaneous reductions in both median R_{sp} and α_{sp} at SGP during the current period relative to the earlier period in the late 1990s (Sect. 3.1.3), but seems inconsistent with the lack of

27009

A multi-year study of lower tropospheric aerosol variability and systematic relationships

J. P. Sherman et al.

Title Page

Abstract

Introduction

Conclusions

References

Tables

Figures

◀

▶

◀

▶

Back

Close

Full Screen / Esc

Printer-friendly Version

Interactive Discussion



change in median α_{sp} at BND, despite reductions in R_{sp} similar in magnitude to those at SGP.

3.4.5 Sub-1 μm scattering fraction and scattering Ångström exponent vs. scattering coefficient

5 Sub-1 μm scattering fraction (R_{sp}) increased slightly with increasing loading for $\sigma_{sp} < 20 \text{ M m}^{-1}$ (Fig. 11) at SGP, BND, and APP for all seasons except spring (and fall at SGP). All three sites demonstrated modest decreases in R_{sp} with further increases in loading ($\sigma_{sp} > 20 \text{ M m}^{-1}$), although the decreases **were** larger for some individual seasons (e.g., winter at BND and SGP). This indicates that conditions of large aerosol loading coincided with a larger contribution from coarse-mode aerosol particles present at these sites. At all three sites, however, coarse mode particles contributed less than half the scattering, even at the highest loadings. Though SGP and BND had very similar mean R_{sp} values for all scattering bins, APP had higher mean R_{sp} values than either SGP or BND over the range of σ_{sp} for all seasons. The R_{sp} at APP also stayed constant until larger σ_{sp} ($\sim 65 \text{ M m}^{-1}$), indicating that the relative contribution of super-1 μm particles to the scattering at APP **was** small and relatively independent of loading over a majority of loading levels at APP. The R_{sp} vs. σ_{sp} relationships for individual seasons at each of the three sites **were** not much different than the respective annual R_{sp} vs. σ_{sp} curve over the range of σ_{sp} values typical for that site and season. With a few exceptions (e.g., winter at SGP), values of R_{sp} along each seasonal curve were within **~ 0.03** of the annual curve values over nearly the entire range of σ_{sp} .

Most of the general features of the R_{sp} vs. σ_{sp} relationships discussed above for SGP, BND, and APP were also present in the α_{sp} vs. σ_{sp} relationships (Fig. 11). A similar lack of sensitivity of α_{sp} to changes in σ_{sp} at SGP and BND was reported by D&O2002, on an annual basis. The similarities in the R_{sp} vs. σ_{sp} and α_{sp} vs. σ_{sp} relationships provide further evidence that α_{sp} serves as a better indicator of relative amounts of coarse and fine mode aerosol than average particle size for the sites in this study. The modest

A multi-year study of lower tropospheric aerosol variability and systematic relationships

J. P. Sherman et al.

Title Page

Abstract

Introduction

Conclusions

References

Tables

Figures

◀

▶

◀

▶

Back

Close

Full Screen / Esc

Printer-friendly Version

Interactive Discussion



seasonal variability in R_{sp} (Fig. 2) would then be consistent with the lack of seasonality in α_{sp} at the sites. The α_{sp} vs. σ_{sp} curves for PM_1 at EGB were not displayed, due to the difficulty in relating PM_1 α_{sp} to fine mode aerosol fraction.

3.4.6 Absorption Ångström exponent vs. scattering Ångström exponent

5 Mean absorption Ångström exponent α_{ap} (450/700 nm), calculated for scattering Ångström exponent α_{sp} (450/700 nm) bin sizes of 0.1 are shown for SGP, BND, and APP in Fig. 12. Absorption Ångström exponent decreased with increasing α_{sp} for all seasons at SGP and BND and during summer at APP and showed little variation with α_{sp} during the other seasons at APP (Fig. 12). Based on the R_{sp} vs. α_{sp} relationships
10 (Sect. 3.4.4 and Fig. 11), most of the higher values of α_{ap} at SGP and BND (coinciding with low α_{sp} values) occurred when there was a larger relative influence by coarse mode aerosol (presumably dust). These occurred during all seasons at SGP, autumn only at BND, and very rarely during any season at APP, as indicated by the number of points in α_{sp} bins below ~ 1.0 (Fig. 12). Based on this, dust appears to have influenced aerosol absorption the most at SGP for all seasons and likely exerted little influence on the absorption at APP. The contribution to absorption by dust in fall at BND could be the result of airborne dust generated during harvesting season. The larger dust influence at SGP, relative to BND, could be due to (1) generally drier conditions in OK than in IL, (2) more unplanted fields near SGP than near BND, where corn and soybean are planted on most fields. Lower values of α_{ap} during non-summer months at all sites generally were near 1 and corresponded to higher α_{sp} values, likely due to an increasing BC contribution to absorption. The higher and nearly constant winter values of α_{ap} at APP (~ 1.2 – 1.3) and insensitivity to α_{sp} (along with high R_{sp} values) also indicate a likely influence of brown carbon to winter absorption at APP, likely from regional wood-burning.
20
25

Summer values of mean α_{ap} were lower than those of other seasons for all α_{sp} bins at BND and APP and for all but the lowest α_{sp} bins at SGP (where dust likely influenced

A multi-year study of lower tropospheric aerosol variability and systematic relationships

J. P. Sherman et al.

Title Page

Abstract

Introduction

Conclusions

References

Tables

Figures

◀

▶

◀

▶

Back

Close

Full Screen / Esc

Printer-friendly Version

Interactive Discussion

absorption). The slopes of the α_{ap} vs. α_{sp} curves indicates that α_{ap} values below 1 during summer coincided with higher fractions of fine-mode aerosol (higher α_{sp}). The curves for individual seasons lie close to the annual curves, with the exceptions of summer at SGP and BND and summer and winter at APP.

3.4.7 Absorption Ångström exponent vs. single-scattering albedo

The individual season α_{ap} vs. ω_0 relationships (Fig. 12) at SGP, BND, and APP were similar to the annual curves for all seasons except summer. The summer curve at BND was also similar the annual BND curve except at high ω_0 . Mean α_{ap} during these seasons remained constant or slightly increased with increasing ω_0 until ω_0 approached 0.90 (specifically the ω_0 bin centered at 0.875), with values near 1.2 ± 0.1 . This was followed by sharp decreases in α_{ap} with further increases in ω_0 . Values above 1 during non-summer month lower ω_0 conditions suggest some contribution from organic carbon and/or dust to the dominant absorption by black carbon (e.g., Cazorla et al., 2013); the α_{ap} vs. α_{sp} and R_{sp} vs. α_{sp} relationships point to dust for SGP and BND and to brown carbon at APP. This occurred most frequently during the non-summer seasons at APP and least frequently at SGP, based on the number of points in ω_0 bins below 0.90.

Some of the same qualitative features were present in the summer curves but mean α_{ap} was lower over the entire ω_0 range (more so for SGP and APP) and values were well below 1 for $\omega_0 > 0.90$ at BND and APP. From the b vs. ω_0 relationships (Fig. 10), the lower mean α_{ap} values at all sites during summer also coincided with lower mean b values. When combined, this indicates that lower mean α_{ap} values were associated with larger, more reflective fine-mode particles. Gyawali et al. (2009) reported a similar α_{ap} vs. ω_0 relationship for summer months without a biomass burning influence in Reno, NV with a near constant $\alpha_{ap} \sim 1.1-1.2$ up to $\omega_0 \sim 0.90$, followed by α_{ap} values mostly below one for higher ω_0 . They attributed this wavelength dependence of absorption to particles coated with non-absorbing organic and inorganic matter. It should be noted that they used a photo-acoustic spectrometer (as compared to the filter-based

A multi-year study of lower tropospheric aerosol variability and systematic relationships

J. P. Sherman et al.

Title Page

Abstract

Introduction

Conclusions

References

Tables

Figures

◀

▶

◀

▶

Back

Close

Full Screen / Esc

Printer-friendly Version

Interactive Discussion



A multi-year study of lower tropospheric aerosol variability and systematic relationships

J. P. Sherman et al.

Title Page

Abstract

Introduction

Conclusions

References

Tables

Figures

◀

▶

◀

▶

Back

Close

Full Screen / Esc

Printer-friendly Version

Interactive Discussion

techniques used at the sites in this study) and **also** used different wavelengths (405 and 870 nm) so the results are not directly comparable. The summer values of α_{ap} at APP were also much lower for all ω_0 than those reported by Gyawali et al. (2009). Possible biases in filter-based absorption measurements made in high-organic aerosol environments could in principle also contribute to this result (e.g., Lack et al., 2008, 2009). A detailed analysis of the effects, both real and artifact, of absorbing and non-absorbing coatings on the wavelength-dependence of light absorption by black carbon is beyond the scope of this paper.

3.4.8 Absorption Ångström exponent vs. scattering coefficient

When studied on an annual basis, mean α_{ap} decreased with increasing aerosol loading at SGP, BND, and APP, with the smallest negative slope at SGP and the largest at APP (Fig. 12). For most non-summer seasons (and even summer at SGP) the mean α_{ap} values at all sites **were** in the range 0.9–1.2 over much of the σ_{sp} range, indicating that much of the absorption during these seasons was likely due to BC. A noticeable exception is winter at APP, where mean α_{ap} was independent of σ_{sp} and the value of ~ 1.3 is indicative of either some dust or brown carbon influence. The high and relatively constant $R_{sp} \sim 0.85$ seems to point to brown carbon, possibly from local and/or regional wood-burning during winter. In contrast, summer α_{ap} at BND and APP was much more sensitive to **loading, in addition to** possessing much lower mean α_{ap} values for all levels of loading than during other seasons. Mean summer α_{ap} values **were** well under 1 for all but the lowest loading conditions at both sites (especially APP), possibly influenced by condensation of organic and/or inorganic material on absorbing cores, as discussed in the previous section.

4 Summary and conclusions

Seasonal variability in scattering, absorption, and most aerosol intensive properties **was** much larger than day of week and diurnal variability at the four North American continental sites studied. Regional differences in annual median properties **were** in general much less than their seasonal variability at individual **sites, requiring** that studies of regional variability be conducted on a seasonal basis. ~~That being said,~~ there **were** regional differences in the relative influence of coarse mode aerosols to scattering and absorption that applied to all **seasons, and hence** on an annual basis as well. Median R_{sp} and R_{ap} **were** higher at APP than at BND and SGP for all months (Figs. 1 and 2), indicating that fine-mode particles contributed more to aerosol light scattering and absorption at APP than at SGP and BND.

Seasonal variability in σ_{sp} was larger than that of σ_{ap} at all sites except EGB (where **their** variability **was** comparable in magnitude), while the opposite **was** true on weekly and diurnal scales. When combined with the seasonal ω_0 vs. σ_{sp} relationships (Fig. 9), this indicates that the sources of σ_{sp} and σ_{ap} were most similar at EGB (primary sources) and most different at APP. The pronounced summer maxima in σ_{sp} observed at all sites was most noticeable at APP and EGB and was accompanied by decreases in b and increases in ω_0 at all **sites, corresponding to larger, more** reflective particles. Median α_{ap} values much less than 1 **were** also observed during summer months at APP, and to a lesser degree BND. **The annual cycle of biogenic VOC emissions and photochemistry likely played an important role in the seasonality of aerosol properties at APP while at EGB it was determined mainly by the frequency of episodic pollution in south/southeasterly flow from the heavily populated southern Ontario and NE US** These claims are supported by studies of aerosol chemistry at EGB (Chan et al., 2010), by aerosol chemistry and VOC measurements made at APP (Link et al., 2014) and by similar seasonality of biogenic VOCs and aerosol optical depth in the SE US (Goldstein et al., 2009). The sources of seasonality at BND and SGP appear to be a combination of photochemistry and patterns in agricultural activity, with less-pronounced σ_{sp} peaks

A multi-year study of lower tropospheric aerosol variability and systematic relationships

J. P. Sherman et al.

Title Page

Abstract

Introduction

Conclusions

References

Tables

Figures

◀

▶

◀

▶

Back

Close

Full Screen / Esc

Printer-friendly Version

Interactive Discussion

during summer months possibly due to lower precursor emissions by vegetation near these sites, as compared to the forests in the SE US.

Large variability in σ_{ap} on weekly timescales (relative to variability in σ_{sp}) **was** likely influenced by regional combustion sources (most likely vehicle emissions) while local and regional traffic and the diurnal cycle in boundary layer height likely contributed to the diurnal variability in σ_{ap} . Sunday and/or Monday minima in median σ_{ap} were observed for all seasons at all sites, with the exception of fall and winter at BND and spring at EGB. The days of minima σ_{ap} and the amplitudes of the weekly σ_{ap} cycles (generally on the order of $\sim 15\text{--}30\%$) are similar to the weekly cycles in BC aerosol mass concentrations at IMPROVE sites in the US reported by Murphy et al. (2008), which they concluded **was** largely influenced by diesel emissions across the US. A lack of weekly and diurnal cycles of most aerosol intensive properties **was** observed for all sites, even when examined for individual seasons. Exceptions include small cycles in ω_0 (larger at EGB) that followed the σ_{ap} cycles. These results indicate that the amount of absorbing aerosol varied on weekly and diurnal timescales much more than the amount of scattering aerosol and that the aerosol size distributions exhibit little change on these timescales.

Large decreases in scattering (especially the PM_{10} component) at BND and SGP for the 2010–2013 period, relative to the 1996–2000 period at BND and 1997–2000 period at SGP reported by D&O2002, are in agreement with those of several other North American studies reporting decreases in aerosol light scattering, extinction, and optical depth (Collaud Coen et al., 2013; Hand et al., 2014; Li et al., 2014; Yoon, 2012). Similar (or even larger) reductions would likely have been observed at APP and EGB, based on the regional difference in aerosol loading trends reported in some of the other studies. Key indicators of aerosol size distribution have also exhibited noticeable changes at BND and SGP since D&O2002. The relative influence of coarse mode aerosols to scattering and absorption has increased at both sites, with declines in accumulation-mode aerosol more likely than increases in dust. The shift to smaller accumulation mode particles (larger b) at both sites could be the result of less growth due to gas-

A multi-year study of lower tropospheric aerosol variability and systematic relationships

J. P. Sherman et al.

Title Page

Abstract

Introduction

Conclusions

References

Tables

Figures

◀

▶

◀

▶

Back

Close

Full Screen / Esc

Printer-friendly Version

Interactive Discussion

A multi-year study of lower tropospheric aerosol variability and systematic relationships

J. P. Sherman et al.

Title Page

Abstract

Introduction

Conclusions

References

Tables

Figures

◀

▶

◀

▶

Back

Close

Full Screen / Esc

Printer-friendly Version

Interactive Discussion

to-particle conversion, given the high sensitivity of b over much of the size range of particles where this conversion is most efficient and the large reductions in gaseous precursors (most notably SO_2 in the US and Canada) in the past two decades.

Sensitivity of mean aerosol intensive properties to aerosol loading was investigated on an annual basis and for individual seasons, along with selected relationships between intensive properties. In addition to their utility in constraining models and for inversions of remote sensing data, these relationships can provide information regarding aerosol sources and processes. Some observed relationships were similar for all seasons at all sites. The aerosols during low loading conditions tended to be smaller and more absorbing (higher b and lower ω_0) for all sites and seasons, consistent with preferential removal of large scattering particles by cloud scavenging and/or deposition. The particles tended to be larger and less absorbing for high loading conditions, consistent with particle growth. Similar relationships were reported by D&O2002 and Andrews et al. (2011). The opposing variations in b and ω_0 resulted in little change in DRFE with loading for all sites and seasons, with exception of moderate seasonal variability in PM_{10} DRFE at EGB. A proportional increase in R_{sp} with increasing α_{sp} , along with a relatively weak relationship between α_{sp} and σ_{sp} , provides evidence that α_{sp} is a better indicator of fine-mode aerosol fraction than particle size at the four sites. The weak seasonal variability of R_{sp} and α_{sp} and larger seasonal variability in b indicates that most of the seasonal changes in size distribution at the four sites were likely in the smaller accumulation-mode particles.

While systematic relationships among most variables were reasonably well-represented by the annual relationships, most involving α_{ap} varied highly with season, both in magnitude and shape of the curves. Mean α_{ap} was much lower during summer months and values below 1 were associated with nearly all loading levels at APP and with higher loading levels at BND. Similar behavior was observed at SGP during fall. Values of $\alpha_{\text{ap}} < 1$ were associated with high ω_0 and higher relative influence from fine-mode aerosols. High ω_0 is associated with smaller b (Fig. 10), leading us to hypothesize condensation of organic and inorganic matter onto BC aerosols as the

source of the observed low α_{ap} during summer months at APP (and to a lesser degree BND), when biogenic emissions and photochemistry are highest. Measurements of sulfate and organic aerosol mass concentrations at APP that support this hypothesis will be the subject of a future publication.

5 **The Supplement related to this article is available online at
doi:10.5194/acpd-14-26971-2014-supplement.**

Acknowledgements. DOE ARM program, NOAA Climate Program Office. Derek Hageman of NOAA-ESRL, Appalachian State University College of Arts and Sciences and all students who participated in data-taking, Michael Link for providing aerosol chemistry figures for APP (located
10 in Supplement to this paper).

References

- Anderson, T. L. and Ogren, J. A.: Determining aerosol radiative properties using the TSI 3563 integrating nephelometer, *Aerosol Sci. Tech.*, 29, 57–69, 1998.
- 15 Anderson, T. L., Covert, D. S., Wheeler, J. D., Harris, J. M., Perry, K. D., Trost, B. E., Jaffe, D. J., and Ogren, J. A.: Aerosol backscatter fraction and single-scattering albedo: measured values and uncertainties at a coastal station in the Pacific Northwest, *J. Geophys. Res.*, 104, 26793–26807, doi:10.1029/1999JD900172, 1999.
- Anderson, T. L., Masonis, S. J., Covert, D. S., Ahlquist, N. C., Howell, S. G., Clarke, A. D., and McNaughton, C. S.: Variability of aerosol optical properties derived from in situ aircraft
20 measurements during ACE-Asia, *J. Geophys. Res.*, 108, 8647, doi:10.1029/2002JD003247, 2003.
- Andreae, M. O., Jones, C. D., and Cox, P. M.: Strong present-day aerosol cooling implies a hot future, *Nature*, 435, 1187–1190, 2005.
- Andrews, E., Sheridan, P. J., Ogren, J. A., and Ferrare, R.: In situ aerosol profiles over the
25 Southern Great Plains cloud and radiation test bed site: 1. Aerosol optical properties, *J. Geophys. Res.*, 109, D06208, doi:10.1029/2003JD004025, 2004.

27017

A multi-year study of lower tropospheric aerosol variability and systematic relationships

J. P. Sherman et al.

Title Page

Abstract

Introduction

Conclusions

References

Tables

Figures

◀

▶

◀

▶

Back

Close

Full Screen / Esc

Printer-friendly Version

Interactive Discussion



A multi-year study of lower tropospheric aerosol variability and systematic relationships

J. P. Sherman et al.

Title Page

Abstract

Introduction

Conclusions

References

Tables

Figures

◀

▶

◀

▶

Back

Close

Full Screen / Esc

Printer-friendly Version

Interactive Discussion

- Andrews, E., Sheridan, P. J., Fiebig, M., McComiskey, A., Ogren, J. A., Arnott, P., Covert, D., Elleman, R., Gasparini, R., Collins, D., Jonsson, H., Schmid, B., and Wang, J.: Comparison of methods for deriving aerosol asymmetry parameter, *J. Geophys. Res.*, 111, D05S04, doi:10.1029/2004JD005734, 2006.
- 5 Andrews, E., Ogren, J. A., Bonasoni, P., Marinoni, A., Cuevas, E., Rodriguez, S., Sun, J. Y., Jaffe, D. A., Fischer, E. V., Baltensperger, U., Weingartner, E., Collaud Coen, M., Sharma, S., Macdonald, A. M., Leaitch, W. R., Lin, N.-H., Laj, P., Arsov, T., Kalapov, I., Jefferson, A., and Sheridan, P.: Climatology of aerosol radiative properties in the free troposphere, *Atmos. Res.*, 102, 365–393, 2011.
- 10 Bergstrom, R. W., Pilewskie, P., Russell, P. B., Redemann, J., Bond, T. C., Quinn, P. K., and Sierau, B.: Spectral absorption properties of atmospheric aerosols, *Atmos. Chem. Phys.*, 7, 5937–5943, doi:10.5194/acp-7-5937-2007, 2007.
- Bond, T. C., Anderson, T. L., and Campbell, D.: Calibration and inter-comparison of filter-based measurements of visible light absorption by aerosols, *Aerosol Sci. Tech.*, 30, 582–600, doi:10.1080/027868299304435, 1999.
- 15 Cazorla, A., Bahadur, R., Suski, K. J., Cahill, J. F., Chand, D., Schmid, B., Ramanathan, V., and Prather, K. A.: Relating aerosol absorption due to soot, organic carbon, and dust to emission sources determined from in-situ chemical measurements, *Atmos. Chem. Phys.*, 13, 9337–9350, doi:10.5194/acp-13-9337-2013, 2013.
- 20 Chan, T. W., Huang, L., Leaitch, W. R., Sharma, S., Brook, J. R., Slowik, J. G., Abbatt, J. P. D., Brickell, P. C., Liggio, J., Li, S.-M., and Moosmüller, H.: Observations of OM/OC and specific attenuation coefficients (SAC) in ambient fine PM at a rural site in central Ontario, Canada, *Atmos. Chem. Phys.*, 10, 2393–2411, doi:10.5194/acp-10-2393-2010, 2010.
- Clarke, A., McNaughton, C., Kapustin, V., Shinozuka, V., Howell, S., Dibb, J., Zhou, J., Anderson, B., Brekhovskikh, V., Turner, H., and Pinkerton, M.: Biomass burning and pollution aerosol over North America: organic components and their influence on spectral optical properties and humidification response, *J. Geophys. Res.*, 112, D12S18, doi:10.1029/2006JD007777, 2007.
- 25 Collaud Coen, M., Weingartner, E., Nyeki, S., Cozic, J., Henning, S., Verheggen, B., Gehrig, R., and Baltensperger, U.: Long-term trend analysis of aerosol variables at the high-alpine site Jungfraujoch, *J. Geophys. Res.*, 112, D13213, doi:10.1029/2006JD007995, 2007.
- 30 Collaud Coen, M., Andrews, E., Asmi, A., Baltensperger, U., Bukowiecki, N., Day, D., Fiebig, M., Fjaeraa, A. M., Flentje, H., Hyvärinen, A., Jefferson, A., Jennings, S. G., Kouvarakis, G.,

A multi-year study of lower tropospheric aerosol variability and systematic relationships

J. P. Sherman et al.

Title Page

Abstract

Introduction

Conclusions

References

Tables

Figures

◀

▶

◀

▶

Back

Close

Full Screen / Esc

Printer-friendly Version

Interactive Discussion

Lihavainen, H., Lund Myhre, C., Malm, W. C., Mihapopoulos, N., Molenaar, J. V., O'Dowd, C., Ogren, J. A., Schichtel, B. A., Sheridan, P., Virkkula, A., Weingartner, E., Weller, R., and Laj, P.: Aerosol decadal trends – Part 1: In-situ optical measurements at GAW and IMPROVE stations, *Atmos. Chem. Phys.*, 13, 869–894, doi:10.5194/acp-13-869-2013, 2013.

5 Costabile, F., Barnaba, F., Angelini, F., and Gobbi, G. P.: Identification of key aerosol populations through their size and composition resolved spectral scattering and absorption, *Atmos. Chem. Phys.*, 13, 2455–2470, doi:10.5194/acp-13-2455-2013, 2013.

Delene, D. J. and Ogren, J. A.: Variability of aerosol optical properties at four North American surface monitoring sites, *J. Atmos. Sci.*, 59, 1135–1150, 2002.

10 Dubovik, O., Smirnov, A., Holben, B. N., King, M. D., Kaufman, Y. J., Eck, T. F., and Slutsker, I.: Accuracy assessments of aerosol optical properties retrieved from Aerosol Robotic Network (AERONET) Sun and sky radiance measurements, *J. Geophys. Res.*, 105, 9791–9806, 2000.

Fast, J., Zhang, Q., Tilp, A., Shippert, T., Parworth, C., and Mei, F.: Organic aerosol component (OACOMP): an ARM value-added product, ARM Climate Science Research Facility report, DOE/SC-ARM-TR-131, available at: https://www.arm.gov/publications/tech_reports/doe-sc-arm-tr-131.pdf (last access: 25 October 2014), 2013.

15 Goldstein, A. H., Koven, C. D., Heald, C. L., and Fung, I. Y.: Biogenic carbon and anthropogenic pollutants combine to form a cooling haze over the southeastern United States, *P. Natl. Acad. Sci. USA*, 106, 8835–8840, doi:10.1073/pnas.0904128106, 2009.

20 Gyawali, M., Arnott, W. P., Lewis, K., and Moosmüller, H.: In situ aerosol optics in Reno, NV, USA during and after the summer 2008 California wildfires and the influence of absorbing and non-absorbing organic coatings on spectral light absorption, *Atmos. Chem. Phys.*, 9, 8007–8015, doi:10.5194/acp-9-8007-2009, 2009.

25 Hand, J. L., Copeland, S. A., McDade, C. E., Day, D. E., Moore Jr., C. T., Dillner, A. M., Pitchford, M. L., Indresand, H., Schichtel, B. A., Malm, W. C., and Watson, J. G.: Spatial and seasonal patterns and temporal variability of haze and its constituents in the United States: Report V, CIRA Report, ISSN: 0737-5352-87, Fort Collins, CO, USA, 2011.

30 Hand, J. L., Schichtel, B. A., Malm, W. C., and Pitchford, M. L.: Particulate sulfate ion concentration and SO₂ emission trends in the United States from the early 1990s through 2010, *Atmos. Chem. Phys.*, 12, 10353–10365, doi:10.5194/acp-12-10353-2012, 2012.

A multi-year study of lower tropospheric aerosol variability and systematic relationships

J. P. Sherman et al.

Title Page

Abstract

Introduction

Conclusions

References

Tables

Figures

◀

▶

◀

▶

Back

Close

Full Screen / Esc

Printer-friendly Version

Interactive Discussion

- Hand, J. L., Schichtel, B. A., Malm, W. C., Copeland, S., Molenaar, J. V., Frank, N., and Pitchford, M.: Widespread reductions in haze across the United States from the early 1990s through 2011, *Atmos. Environ.*, 94, 671–679, doi:10.1016/j.atmosenv.2014.05.062, 2014.
- Hansen, J., Sato, M., and Ruedy, R.: Radiative forcing and climate response, *J. Geophys. Res.*, 102, 6831–6864, 1997.
- Haywood, J. M. and Shine, K. P.: The effect of anthropogenic sulfate and soot aerosol on the clear sky planetary radiation budget, *Geophys. Res. Lett.*, 22, 603–606, doi:10.1029/95GL00075, 1995.
- Holben, B. N., Eck, T. F., Slutsker, I., Tanre, D., Buis, J. P., Setzer, A., Vermote, E., Reagan, J. A., Kaufman, Y. J., Nakajima, T., Lavenu, F., Janowiak, I., and Smirnov, A.: AERONET – a federated instrument network and data archive for aerosol characterization, *Remote Sens. Environ.*, 66, 1–16, 1998.
- Kahn, R. A., Yu, H., Schwartz, S. E., Chin, M., Feingold, G., Remer, L. A., Rind, D., Halthore, R., and DeCola, P.: Introduction, in: *Atmospheric Aerosol Properties and Climate Impacts*, A Report by the US Climate Change Science Program and the Subcommittee on Global Change Research, edited by: Chin, M., Kahn, R. A., and Schwartz, S. E., National Aeronautics and Space Administration, Washington DC, USA, 9–20, 2009.
- Kleinman, L. I., Daum, P. H., Lee, Y., Senum, G. I., Springston, S. R., Wang, J., Berkowitz, C., Hubbe, J., Zaveri, R. A., Brechtel, F. J., Jayne, J., Onasch, T. B., and Worsnop, D.: Aircraft observations of aerosol composition and ageing in New England and Mid-Atlantic States during the summer 2002 New England Air Quality Study field campaign, *J. Geophys. Res.*, 112, D09310, doi:10.1029/2006JD007786, 2007.
- Kohler, C. H., Trautmann, T., Lindermeier, E., Vreeling, W., Lieke, K., Kandler, K., Weinzierl, B., Groß, S., Tesche, M., and Wendisch, M.: Thermal IR radiative properties of mixed mineral dust and biomass aerosol during SAMUM-2, *Tellus B*, 63, 751–769, doi:10.1111/j.1600-0889.2011.00563.x, 2011.
- Koloutsou-Vakakis, S., Carrico, C. M., Kus, P., Rood, M. J., Li, Z., Shrestha, R., Ogren, J. A., Chow, J. C., and Watson, J. G.: Aerosol properties at a midlatitude Northern Hemisphere continental site, *J. Geophys. Res.*, 106, 3019–3032, doi:10.1029/2000JD900126, 2001.
- Lack, D. A., Cappa, C. D., Covert, D. S., Baynard, T., Massoli, P., Sierau, B., Bates, T. S., Quinn, P. K., Lovejoy, E. R., and Ravishankara, A. R.: Bias in filter-based aerosol light absorption measurements due to organic aerosol loading: evidence from ambient measurements, *Aerosol Sci. Tech.*, 42, 1033–1041, doi:10.1080/02786820802389277, 2008.

**A multi-year study of
lower tropospheric
aerosol variability
and systematic
relationships**

J. P. Sherman et al.

Title Page

Abstract

Introduction

Conclusions

References

Tables

Figures

◀

▶

◀

▶

Back

Close

Full Screen / Esc

Printer-friendly Version

Interactive Discussion



Lack, D. A., Cappa, C. D., Cross, E. S., Massoli, P., Ahern, A. T., Davidovits, P., and Onasch, T. B.: Absorption enhancement of coated absorbing aerosols: validation of the photo-acoustic technique for measuring the enhancement, *Aerosol Sci. Tech.*, 43, 1006–1012, doi:10.1080/02786820903117932, 2009.

5 Levy, R. C., Remer, L. A., Kleidman, R. G., Mattoo, S., Ichoku, C., Kahn, R., and Eck, T. F.: Global evaluation of the Collection 5 MODIS dark-target aerosol products over land, *Atmos. Chem. Phys.*, 10, 10399–10420, doi:10.5194/acp-10-10399-2010, 2010.

Li, J., Carlson, B. E., Dubovik, O., and Laciš, A. A.: Recent trends in aerosol optical properties derived from AERONET measurements, *Atmos. Chem. Phys. Discuss.*, 14, 14351–14397, doi:10.5194/acpd-14-14351-2014, 2014.

10 Link, M. F., Zhou, Y., Taubman, B. F., Sherman, J. P., Sive, B. C., Morrow, H., Krintz, I., Robertson, L., Cook, R., Stocks, J., and West, M.: Estimating background secondary organic aerosol in the southeastern United States from a regionally representative site, *J. Atmos. Chem.*, submitted, 2014.

15 Malm, W. C., Schichtel, B. A., Pitchford, M. L., Ashbaugh, L. L., and Eldred, R. A.: Spatial and monthly trends in speciated fine particle concentration in the United States, *J. Geophys. Res.*, 109, D03306, doi:10.1029/2003JD003739, 2004.

Massoli, P., Murphy, D. M., Lack, D. A., Baynard, T., Brock, C. A., and Lovejoy, E. R.: Uncertainty in light scattering measurements by TSI nephelometer: results from laboratory studies and implications for ambient measurements, *Aerosol Sci. Tech.*, 43, 1064–1074, doi:10.1080/02786820903156542, 2009.

20 Murphy, D. M., Capps, S. L., Daniel, J. S., Frost, G. J., and White, W. H.: Weekly patterns of aerosol in the United States, *Atmos. Chem. Phys.*, 8, 2729–2739, doi:10.5194/acp-8-2729-2008, 2008.

25 Murphy, D. M., Chow, J. C., Leibensperger, E. M., Malm, W. C., Pitchford, M., Schichtel, B. A., Watson, J. G., and White, W. H.: Decreases in elemental carbon and fine particle mass in the United States, *Atmos. Chem. Phys.*, 11, 4679–4686, doi:10.5194/acp-11-4679-2011, 2011.

Ogren, J. A.: Comment on “Calibration and Intercomparison of Filter-Based Measurements of Visible Light Absorption by Aerosols”, *Aerosol Sci. Tech.*, 44, 589–591, doi:10.1080/02786826.2010.482111, 2010.

30 Ogren, J. A., Wendell, J., Sheridan, P. J., Hageman, D., and Jefferson, A.: Continuous light absorption photometer performance, ASR Science Team Meeting, Potomac, Md, USA, 18–21

A multi-year study of lower tropospheric aerosol variability and systematic relationships

J. P. Sherman et al.

Title Page

Abstract

Introduction

Conclusions

References

Tables

Figures

◀

▶

◀

▶

Back

Close

Full Screen / Esc

Printer-friendly Version

Interactive Discussion

March, available at: <http://asr.science.energy.gov/meetings/stm/posters/view?id=781> (last access: 26 October 2014), 2013.

Quinn, P. K., Bates, T. S., Baynard, T., Clarke, A. D., Onasch, T. B., Wang, W., Rood, M., Andrews, E., Allan, J., Carrico, C. M., Coffman, D., and Worsnop, D.: Impact of particulate organic matter on the relative humidity dependence of light scattering: a simplified parameterization, *Geophys. Res. Lett.*, 32, L22809, doi:10.1029/2005GL024322, 2005.

Remer, L. A. and Kaufman, Y. J.: Dynamic aerosol model: urban/industrial aerosol, *J. Geophys. Res.*, 103, 13859–13871, 1998.

Schuster, G. L., Dubovik, O., and Holben, B. N.: Angstrom exponent and bimodal aerosol size distributions, *J. Geophys. Res.*, 111, D07207, doi:10.1029/2005JD006328, 2006.

Seinfeld, J. H. and Pandis, S. N.: *Atmospheric Chemistry and Physics: From Air Pollution to Climate Change*, 2nd edn., John Wiley & Sons, New York, New York, USA, 1998.

Sheridan, P. J. and Ogren, J. A.: Observations of the vertical and regional variability of aerosol optical properties over central and eastern North America, *J. Geophys. Res.*, 104, 16793–16805, doi:10.1029/1999JD900241, 1999.

Sheridan, P. J., Delene, D. J., and Ogren, J. A.: Four years of continuous surface aerosol measurements from the Department of Energy's Atmospheric Radiation Measurement Program Southern Great Plains Cloud and Radiation Testbed site, *J. Geophys. Res.*, 106, 20735–20747, doi:10.1029/2001JD000785, 2001.

Sheridan, P. J., Jefferson, A., and Ogren, J. A.: Spatial variability of submicrometer aerosol radiative properties over the Indian Ocean during INDOEX, *J. Geophys. Res.*, 107, 8011, doi:10.1029/2000JD000166, 2002.

Sheridan, P. J., Andrews, E., Ogren, J. A., Tackett, J. L., and Winker, D. M.: Vertical profiles of aerosol optical properties over central Illinois and comparison with surface and satellite measurements, *Atmos. Chem. Phys.*, 12, 11695–11721, doi:10.5194/acp-12-11695-2012, 2012.

U.S. Environmental Protection Agency: Health Assessment Document for Diesel Engine Exhaust, National Center for Environmental Assessment, Washington DC, EPA/600/8-90/057F, available at: <http://www.epa.gov/ncea> (access date: 26 October 2014), 2002.

van de Hulst, H. C.: *Light Scattering by Small Particles*, John Wiley and Sons, New York, 1957.

Wiscombe, W. J. and Grams, G. W.: The backscattered fraction in two-stream approximations, *J. Atmos. Sci.*, 33, 2440–2451, 1976.

A multi-year study of lower tropospheric aerosol variability and systematic relationships

J. P. Sherman et al.

Title Page

Abstract

Introduction

Conclusions

References

Tables

Figures

◀

▶

◀

▶

Back

Close

Full Screen / Esc

Printer-friendly Version

Interactive Discussion



- Yoon, J., von Hoyningen-Huene, W., Kokhanovsky, A. A., Vountas, M., and Burrows, J. P.: Trend analysis of aerosol optical thickness and Ångström exponent derived from the global AERONET spectral observations, *Atmos. Meas. Tech.*, 5, 1271–1299, doi:10.5194/amt-5-1271-2012, 2012.
- 5 Yu, H., Kaufman, Y. J., Chin, M., Feingold, G., Remer, L. A., Anderson, T. L., Balkanski, Y., Bellouin, N., Boucher, O., Christopher, S., DeCola, P., Kahn, R., Koch, D., Loeb, N., Reddy, M. S., Schulz, M., Takemura, T., and Zhou, M.: A review of measurement-based assessments of the aerosol direct radiative effect and forcing, *Atmos. Chem. Phys.*, 6, 613–666, doi:10.5194/acp-6-613-2006, 2006.
- 10 Yu, H., Quinn, P. K., Feingold, G., Remer, L. A., Kahn, R. A., Chin, M., and Schwartz, S. E.: Remote sensing and in situ measurements of aerosol properties, burdens, and radiative forcing, in: *Atmospheric Aerosol Properties and Climate Impacts*, a Report by the US Climate Change Science Program and the Subcommittee on Global Change Research, edited by: Chin, M., Kahn, R. A., and Schwartz, S. E., National Aeronautics and Space Administration, Washington DC, USA, 21–54, 2009.
- 15 Zhang, X., Hecobian, A., Zheng, M., Frank, N. H., and Weber, R. J.: Biomass burning impact on $PM_{2.5}$ over the southeastern US during 2007: integrating chemically speciated FRM filter measurements, MODIS fire counts and PMF analysis, *Atmos. Chem. Phys.*, 10, 6839–6853, doi:10.5194/acp-10-6839-2010, 2010.

A multi-year study of lower tropospheric aerosol variability and systematic relationships

J. P. Sherman et al.

Title Page

Abstract

Introduction

Conclusions

References

Tables

Figures

◀

▶

◀

▶

Back

Close

Full Screen / Esc

Printer-friendly Version

Interactive Discussion



Table 1. Parameters and equations used to calculate aerosol optical properties. Constants and parameters used in the formula to calculate globally-averaged top-of-atmosphere direct radiative forcing (DRFE) are also included and are denoted with *.

Parameter	Equation (or value)
Extinction coefficient	$\sigma_{\text{ep}} = \sigma_{\text{sp}} + \sigma_{\text{ap}}$
Single-scattering albedo	$\omega_0 = \sigma_{\text{sp}} / \sigma_{\text{ep}} = \sigma_{\text{sp}} / (\sigma_{\text{sp}} + \sigma_{\text{ap}})$
Hemispheric backscatter fraction	$b = \sigma_{\text{bsp}} / \sigma_{\text{sp}}$
Scattering Ångström exponent	$\alpha_{\text{sp}} = -\log(\sigma_{\text{sp}}(\lambda_1) / \sigma_{\text{sp}}(\lambda_2)) / \log(\lambda_1 / \lambda_2)$
Absorption Ångström exponent	$\alpha_{\text{ap}} = -\log(\sigma_{\text{ap}}(\lambda_1) / \sigma_{\text{ap}}(\lambda_2)) / \log(\lambda_1 / \lambda_2)$
Sub-micron scattering fraction	$R_{\text{sp}} = \sigma_{\text{sp,PM}_1} / \sigma_{\text{sp,PM}_{10}}$
Sub-micron absorption fraction	$R_{\text{ap}} = \sigma_{\text{ap,PM}_1} / \sigma_{\text{ap,PM}_{10}}$
Direct Radiative Forcing Efficiency	$\text{DRFE} = \text{DRF} / \tau = -\text{DS}_0 T_{\text{atm}}^2 (1 - A_c) \beta \omega_0 \times \left[(1 - R_s)^2 - (2R_s / \omega_0 \beta) (1 - \omega_0) \right]$
Upscatter Fraction*	$\beta = 0.0817 + 1.8495 \times b - 2.9682 \times b^2$
Fractional Day Length*	$D = 0.50$ (globally-averaged)
Solar Constant*	$S_0 = 1370 \text{ W m}^{-2}$
Atmospheric Transmission*	$T_{\text{atm}} = 0.76$ (globally-averaged)
Cloud Fraction*	$A_c = 0.60$ (globally-averaged)
Spectrally-averaged surface albedo**	$R_s = 0.15$ (globally-averaged)

A multi-year study of lower tropospheric aerosol variability and systematic relationships

J. P. Sherman et al.

Table 2. Sites, instruments and data period included in the study, listed from west to east. Aerosol sampling size cuts and the instrument used to measure absorption is also included. All sites used a TSI 3563 3- λ nephelometer¹ to measure total scattering and hemispheric backscattering.

Site	Lat/Long (°)	Elev. (m a.s.l.)	Yrs. Data used	#Hrs used 2010–2013	Size Cut (μm)	Absorption Instrument (Dates used)
SGP	36.6° N, 97.5° W	315	1997–2013	32 971 (σ_{sp}), 25 140 (σ_{ap})	1.10	1- λ PSAP ² (Apr 1997–Mar 2005), 3- λ PSAP ³ (Apr 2005–Dec 2013)
BND	40.0° N, 88.4° W	230	1996–2013	33 449 (σ_{sp}), 32 040 (σ_{ap})	1.10	1- λ PSAP (Sep 1996–Feb 2006), 3- λ PSAP (Mar 2006–Feb 2012), 3- λ CLAP ⁴ (Mar 2012–Dec 2013)
EGB	44.2° N, 79.8° W	253	2010–2013	32 448 (σ_{sp}), 26 304 (σ_{ap})	1	1- λ PSAP
APP	36.2° N, 81.7° W	1080	2010–2013	34 220 (σ_{sp}), 34 178 (σ_{ap})	1.10	3- λ PSAP

¹ 3- λ TSI nephelometer measures at $\lambda = 450, 550, 700$ nm.

² 1- λ PSAP measures at 565 nm, adjusted to 550 nm using Bond et al. (1999) correction.

³ 3- λ PSAP measures at 467, 530, 660 nm.

⁴ 3- λ CLAP measures at 467, 529, 653 nm.

A multi-year study of lower tropospheric aerosol variability and systematic relationships

J. P. Sherman et al.

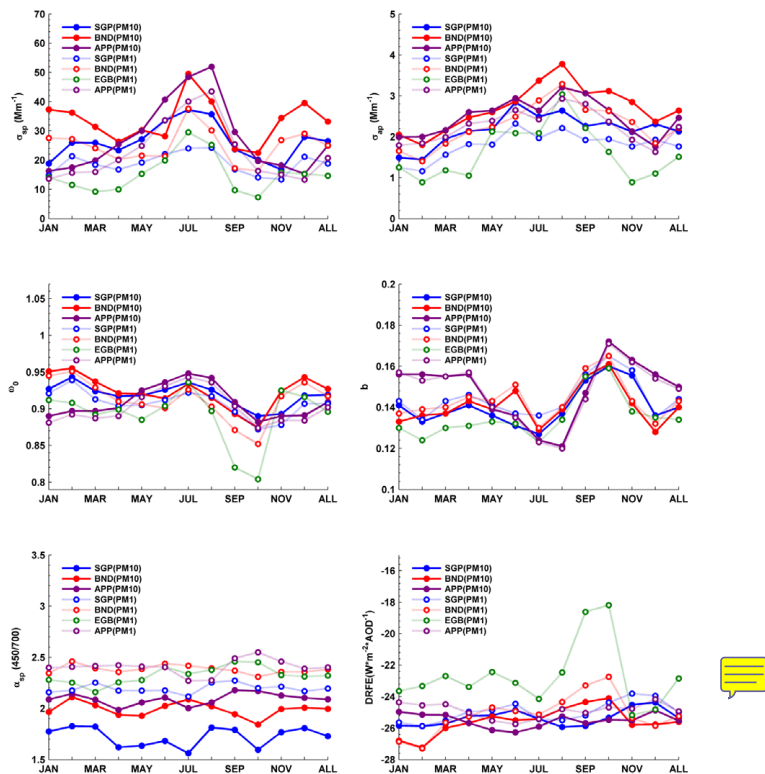


Figure 1. Annual cycle of median PM_{10} and PM_1 aerosol light scattering coefficient (σ_{sp}), absorption coefficient (σ_{ap}), single-scattering albedo (ω_0), hemispheric backscatter fraction (b), scattering Ångström exponent (α_{sp}) and direct radiative forcing efficiency (DRFE) at SGP, BND, APP, and EGB (PM_1 only) for years 2010–2013. The values corresponding to “ALL” are median values for the entire 2010–2013 period (all months). All displayed quantities are for wavelength of 550 nm except for α_{sp} , which is calculated using the 450 and 700 nm wavelengths.

Title Page

Abstract

Introduction

Conclusions

References

Tables

Figures

◀

▶

◀

▶

Back

Close

Full Screen / Esc

Printer-friendly Version

Interactive Discussion

A multi-year study of lower tropospheric aerosol variability and systematic relationships

J. P. Sherman et al.

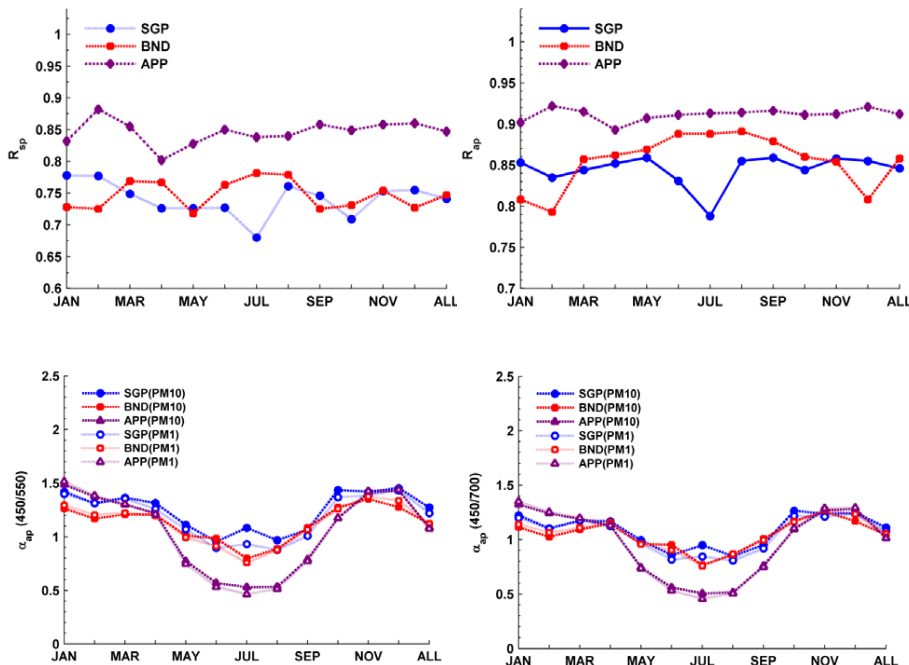


Figure 2. Annual cycle of median sub-1 μm aerosol scattering and absorption fractions (R_{sp} and R_{ap}) at 550 nm, along with median PM_{10} and PM_1 aerosol absorption Ångström exponents (α_{ap}), using the 450/550 nm and 450/700 nm pairs, for years 2010–2013. The values corresponding to “ALL” are median values for the entire 2010–2013 period (all months).

Title Page

Abstract Introduction

Conclusions References

Tables Figures

◀ ▶

◀ ▶

Back Close

Full Screen / Esc

Printer-friendly Version

Interactive Discussion



A multi-year study of lower tropospheric aerosol variability and systematic relationships

J. P. Sherman et al.

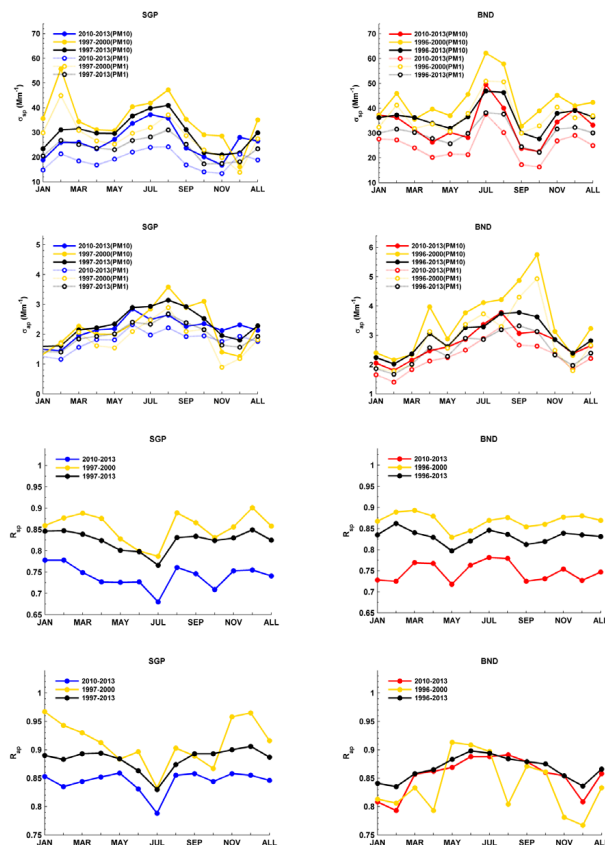


Figure 3. Annual cycle of median PM_{10} and PM_1 aerosol light scattering coefficient (σ_{sp}), absorption coefficient (σ_{ap}), and sub-micrometer scattering and absorption fractions (R_{sp} and R_{ap} , respectively) at 550 nm at SGP and BND for different periods. Data points corresponding to “ALL” are median values over the entire period.

A multi-year study of lower tropospheric aerosol variability and systematic relationships

J. P. Sherman et al.

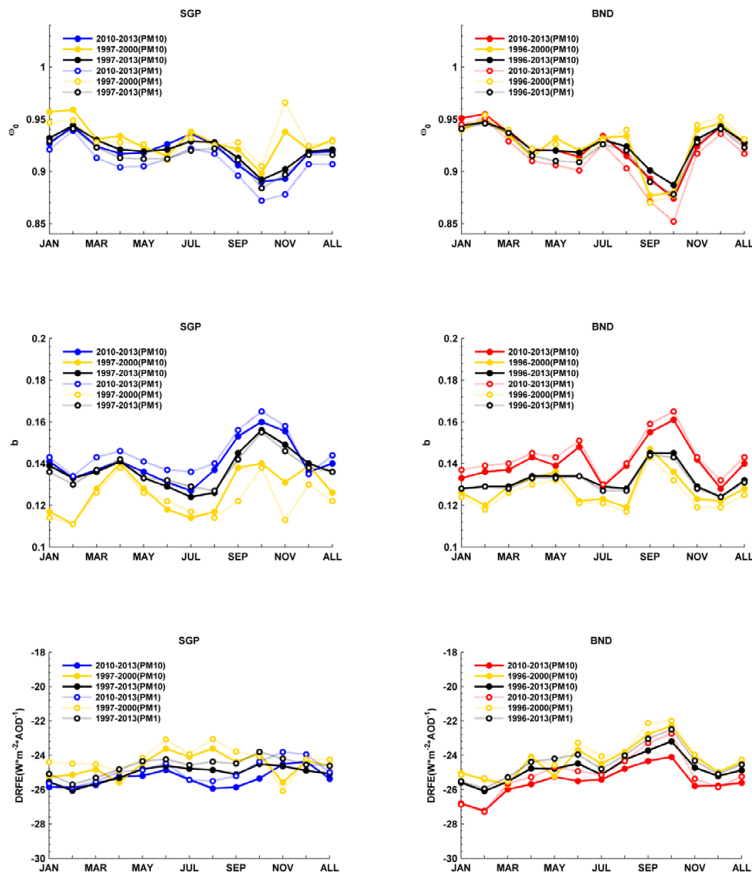


Figure 4. Annual cycle of median PM_{10} and PM_1 aerosol single-scattering albedo (ω_0), hemispheric backscatter coefficient (b), and direct radiative forcing efficiency (DRFE) at 550 nm at SGP and BND for different periods. The values corresponding to “ALL” are median values over the entire period.

[Title Page](#)
[Abstract](#)
[Introduction](#)
[Conclusions](#)
[References](#)
[Tables](#)
[Figures](#)
[Back](#)
[Close](#)
[Full Screen / Esc](#)
[Printer-friendly Version](#)
[Interactive Discussion](#)

A multi-year study of lower tropospheric aerosol variability and systematic relationships

J. P. Sherman et al.

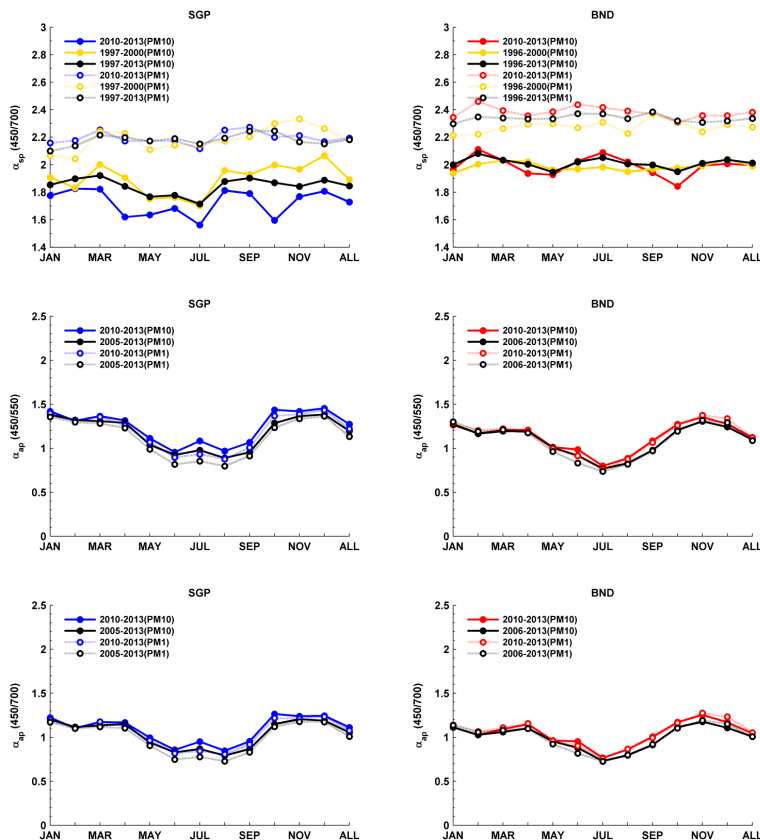


Figure 5. Annual cycle of median PM₁₀ and PM₁ aerosol scattering and absorption Ångström exponent (α_{sp} , and α_{ap}), at SGP and BND for different periods, calculated using the wavelengths (in nm) denoted on y axis. The values corresponding to “ALL” are median values over the entire period. The 3- λ absorption measurements were initiated in 2005 at SGP and 2006 at BND so no comparisons with D&O2002 are available for α_{ap} .

Title Page

Abstract

Introduction

Conclusions

References

Tables

Figures

◀

▶

◀

▶

Back

Close

Full Screen / Esc

Printer-friendly Version

Interactive Discussion



A multi-year study of lower tropospheric aerosol variability and systematic relationships

J. P. Sherman et al.

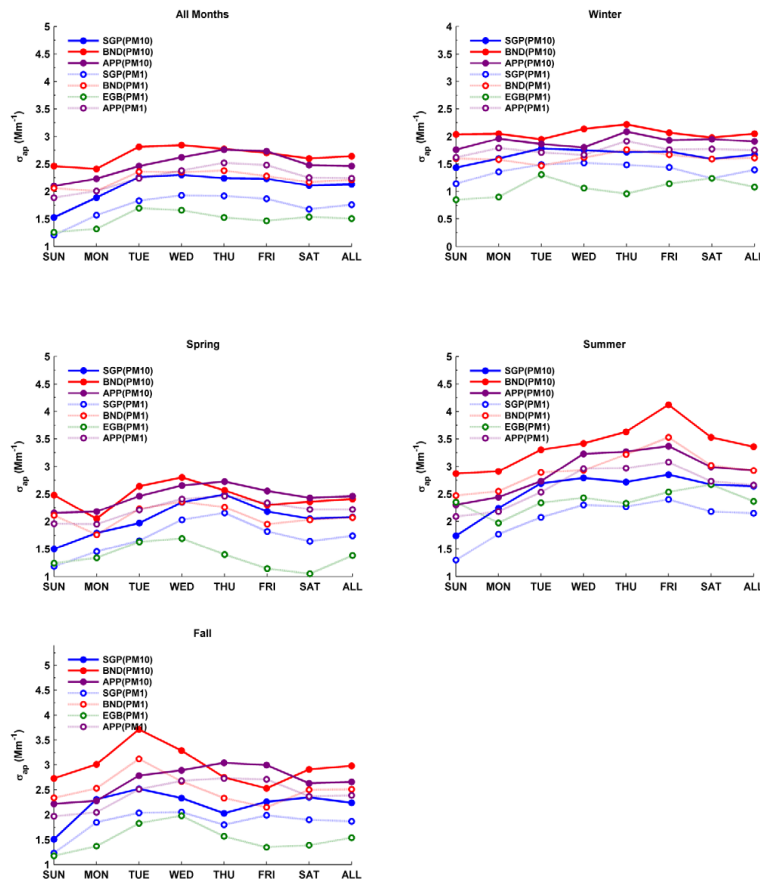


Figure 6. Weekly cycle of median PM_{10} and PM_1 aerosol absorption coefficient (σ_{ap}) at 550 nm for full years (all months) and broken down by season, over the period 2010–2013. Months comprising the seasons are DJF (winter), MAM (spring), JJA (summer), and SON (fall). The values corresponding to “ALL” are median values over the entire period for that particular season.

Title Page

Abstract

Introduction

Conclusions

References

Tables

Figures

◀

▶

◀

▶

Back

Close

Full Screen / Esc

Printer-friendly Version

Interactive Discussion

A multi-year study of lower tropospheric aerosol variability and systematic relationships

J. P. Sherman et al.

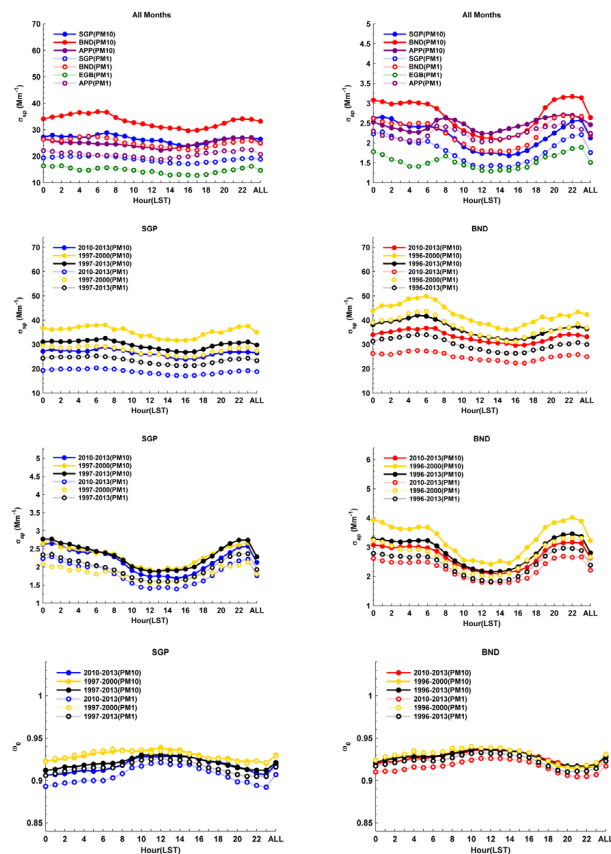


Figure 7. Diurnal cycle of median PM_{10} and PM_1 aerosol light scattering coefficient (σ_{sp}) and absorption coefficient (σ_{ap}) at 550 nm for all months of the 2010–2013 period at a site, along with median σ_{sp} , σ_{ap} , and single-scattering albedo (ω_0) at 550 nm for different periods at SGP and BND. The values corresponding to “ALL” are median values over the entire period.

A multi-year study of lower tropospheric aerosol variability and systematic relationships

J. P. Sherman et al.

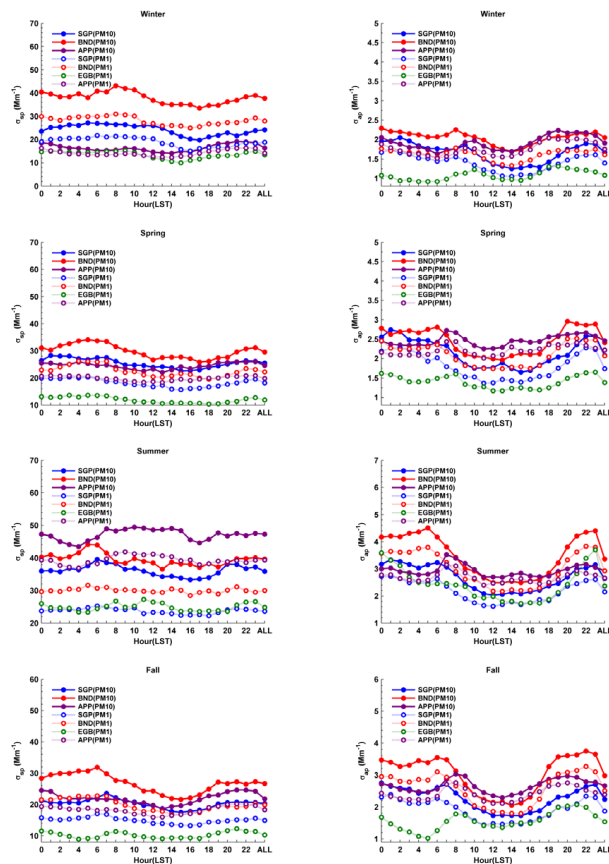


Figure 8. Diurnal cycle of median PM_{10} and PM_1 aerosol scattering coefficient (σ_{sp}) and absorption coefficient (σ_{ap}) at 550 nm for all sites, broken down by individual seasons, during the period 2010–2013. Months comprising the seasons are DJF (winter), MAM (spring), JJA (summer), and SON (fall). The values corresponding to “ALL” are median values over the given seasons for the entire period.

Title Page	
Abstract	Introduction
Conclusions	References
Tables	Figures
◀	▶
◀	▶
Back	Close
Full Screen / Esc	
Printer-friendly Version	
Interactive Discussion	

A multi-year study of lower tropospheric aerosol variability and systematic relationships

J. P. Sherman et al.

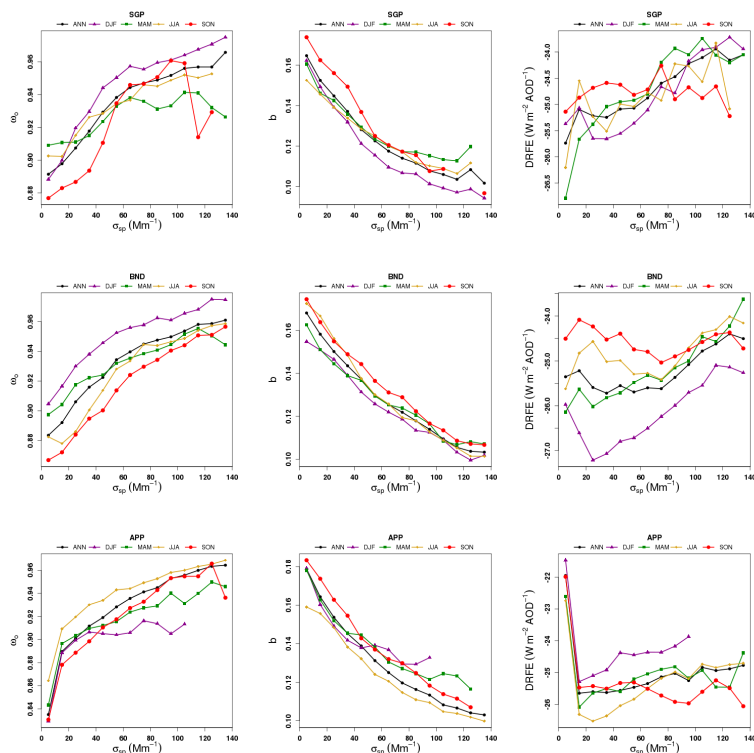


Figure 9. Mean single-scattering albedo (ω_0), hemispheric backscatter fraction (b), and direct radiative forcing efficiency (DRFE) vs. aerosol light scattering coefficient (σ_{sp}) for individual seasons and full annual cycles at SGP, BND, EGB, and APP over the years 2010–2013. Months comprising the seasons are DJF (winter), MAM (spring), JJA (summer), and SON (fall). The “ANN” curve in each plot represents the curve for all seasons. The mean values were calculated over $10 \text{ M m}^{-1} \sigma_{sp}$ bins. All displayed quantities are for wavelength of 550 nm. Displayed curves are for PM_{10} at SGP, BND, and APP and for PM_1 at EGB.

Title Page

Abstract

Introduction

Conclusions

References

Tables

Figures

◀

▶

◀

▶

Back

Close

Full Screen / Esc

Printer-friendly Version

Interactive Discussion

A multi-year study of lower tropospheric aerosol variability and systematic relationships

J. P. Sherman et al.

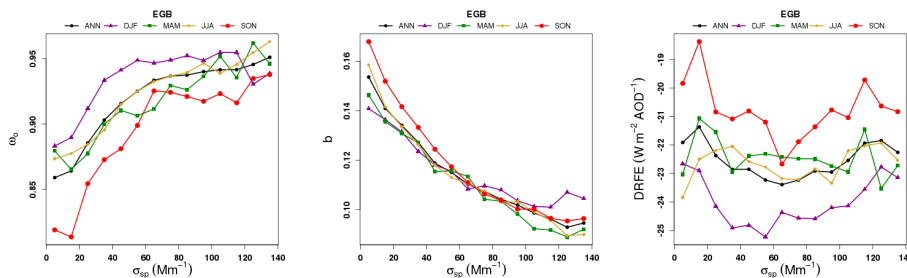


Figure 9. Continued.

Title Page	
Abstract	Introduction
Conclusions	References
Tables	Figures
◀	▶
◀	▶
Back	Close
Full Screen / Esc	
Printer-friendly Version	
Interactive Discussion	



A multi-year study of lower tropospheric aerosol variability and systematic relationships

J. P. Sherman et al.

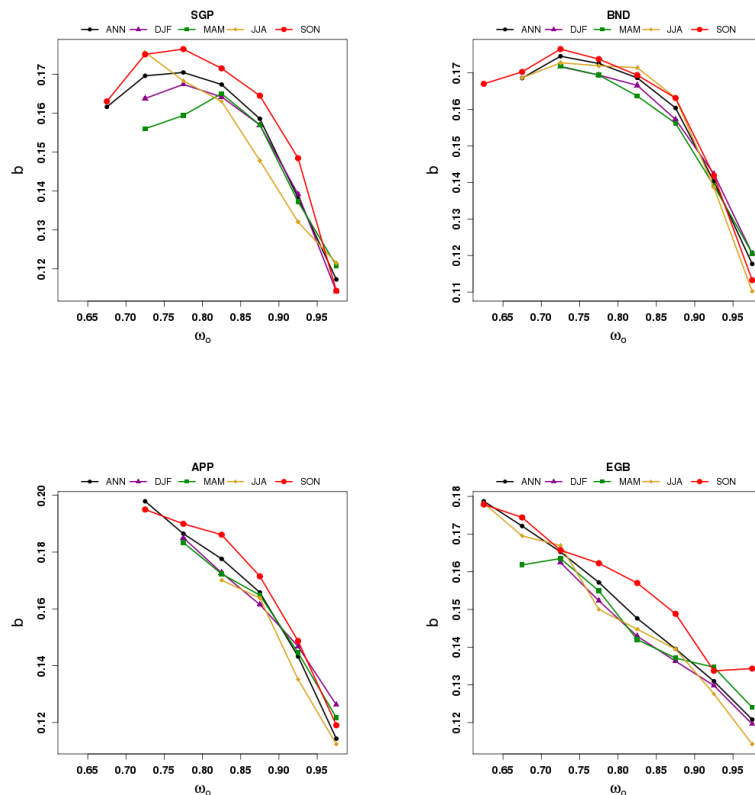


Figure 10. Mean hemispheric backscatter fraction (b) vs. single scattering albedo (ω_0) for individual seasons and full annual cycles at SGP, BND, APP, and EGB over the years 2010–2013. Months comprising the seasons are DJF (winter), MAM (spring), JJA (summer), and SON (fall). The “ANN” curve in each plot represents the curve for all seasons. Displayed curves are for PM_{10} at SGP, BND, and APP and for PM_1 at EGB. The mean values were calculated over $10 \text{ M m}^{-1} \sigma_{\text{sp}}$ bins and over $0.05 \omega_0$ bins. All displayed quantities are for wavelength of 550 nm .

[Title Page](#)
[Abstract](#)
[Introduction](#)
[Conclusions](#)
[References](#)
[Tables](#)
[Figures](#)
[◀](#)
[▶](#)
[◀](#)
[▶](#)
[Back](#)
[Close](#)
[Full Screen / Esc](#)
[Printer-friendly Version](#)
[Interactive Discussion](#)

A multi-year study of lower tropospheric aerosol variability and systematic relationships

J. P. Sherman et al.

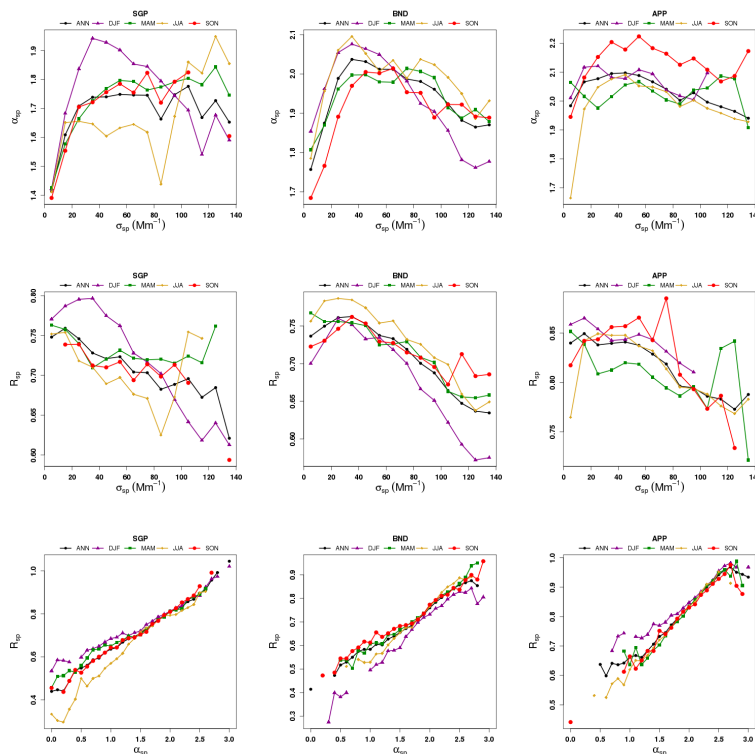


Figure 11. Mean scattering Ångström exponent (α_{sp}) and sub-micrometer scattering fraction (R_{sp}) vs. scattering coefficient (σ_{sp}) and mean R_{sp} vs. α_{sp} for individual seasons and full annual cycles at SGP, BND, and APP over the years 2010–2013. Months comprising the seasons are DJF (winter), MAM (spring), JJA (summer), and SON (fall). The “ANN” curve in each plot represents the curve for all seasons. The mean values were calculated over $10 Mm^{-1}$ σ_{sp} bins and over $0.1 \alpha_{sp}$ bins. All values are for the PM_{10} size cut. R_{sp} and σ_{sp} are given for a wavelength of 550 nm and α_{sp} and α_{ap} are calculated using the 450/700 nm wavelength pair.

A multi-year study of lower tropospheric aerosol variability and systematic relationships

J. P. Sherman et al.

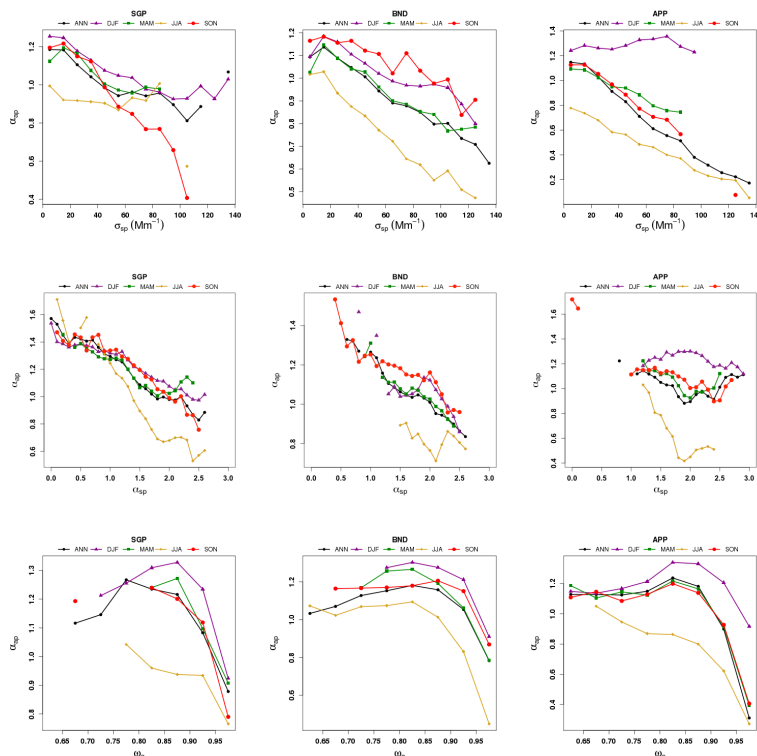


Figure 12. Mean absorption Ångström exponent (α_{ap}) vs. scattering coefficient (σ_{sp}), scattering Ångström exponent (α_{sp}), and single-scattering albedo (ω_0) for individual seasons and full annual cycles at SGP, BND, and APP over the years 2010–2013. Months comprising the seasons are DJF (winter), MAM (spring), JJA (summer), and SON (fall). The “ANN” curve in each plot represents the curve for all seasons. The mean α_{ap} values were calculated over 10 M m^{-1} σ_{sp} bins, $0.1 \alpha_{sp}$ bins, and $0.05 \omega_0$ bins. All values for σ_{sp} and ω_0 are given for a wavelength of 550 nm and α_{sp} and α_{ap} are calculated using the 450/700 nm wavelength pair.

Title Page

Abstract

Introduction

Conclusions

References

Tables

Figures



Back

Close

Full Screen / Esc

Printer-friendly Version

Interactive Discussion

